# BACTERIAL COMMUNITY STRUCTURE IN THE AMUNDSEN SEA POLYNYA, ANTARCTICA

by

#### SIERRA BARTLETT

(Under the Direction of Patricia Yager and Holly Bik)

#### **ABSTRACT**

This study used ocean observations, 16 rRNA, and taxonomic insights to understand the relationships between meltwater-modified ocean circulation, iron supply, and pelagic bacterial community structure in the Amundsen Sea Polynya (ASP), Antarctica. Polynyas are marine ecosystems characterized by seasonal sea ice cover and massive phytoplankton blooms; the ASP is one of the most productive polynyas globally. Ocean models of the ASP suggest the importance of an "iron conveyor belt," comprising iron-rich deepwater upwelled via meltwater entrainment under ice-shelf cavities, delivering key micronutrients to the phytoplankton. How the microbial community changes along this "conveyor belt," and the influence of bacteria on the bioavailability of the iron, was yet to be explored. This research found distinct communities in each water mass, characterized by location within the ASP, suggesting community succession along the route. Aerobic decomposers dominated in the surface waters, within and below the bloom, while bottom-water communities included known siderophore producers. Communities likely performing nitrification and sulfur-oxidization were found near the ice shelf. Our findings indicate a possible coupling of the nitrogen and iron cycle in this system.

INDEX WORDS: Environmental microbiology, Antarctica, coastal polynyas, 16s rRNA.

# BACTERIAL COMMUNITY STRUCTURE IN THE AMUNDSEN SEA POLYNYA, ANTARCTICA

by

# SIERRA BARTLETT

BS, Georgia Southern University, 2021

A Thesis Submitted to the Graduate Faculty of The University of Georgia in Partial Fulfillment of the Requirements for the Degree

MASTER OF SCIENCE

ATHENS, GEORGIA

2024

© 2024

Sierra Bartlett

All Rights Reserved

# BACTERIAL COMMUNITY STRUCTURE IN THE AMUNDSEN SEA POLYNYA, ANTARCTICA

by

# SIERRA BARTLETT

Major Professors: Patricia Yager

Holly Bik

Committee: Jaclyn Saunders

Electronic Version Approved:

Ron Walcott Vice Provost for Graduate Education and Dean of the Graduate School The University of Georgia December 2024

# **DEDICATION**

For Mary, who was my internship mom, a good friend, and an even better scientist. Also, for Kaitlyn, who kept me sane throughout this process.

#### **ACKNOWLEDGEMENTS**

I want to acknowledge the many members of the Bik lab for their help with the wet lab and statistics: Tiago for the significant help with the wet lab and R code, Mirayana for the wet lab and organizational skills, and Hunter and Alejandro for their help with QIIME code. My research was supported by a Graduate Research Assistantship funded by NSF 1941483 - NSFGEO-NERC: Collaborative Research: Accelerating Thwaites Ecosystem Impacts for the Southern Ocean (ARTEMIS) to Dr. Patricia Yager. We thank the United States Antarctic Program (USAP), including the captain, crew, and science team onboard the *RV Nathaniel B*. *Palmer* (NBP) 22-02 for field support. We also thank Dr. Wade H. Jeffrey (University of West Florida) for sharing his filtration supplies when ours were lost during shipping.

# TABLE OF CONTENTS

		Page
ACKNO	WLEDGEMENTS	V
SECTION	NS	
1	INTRODUCTION	1
2	METHODS	6
3	RESULTS	12
4	DISCUSSION	19
5	FIGURES	26
6	TABLES	41
APPEND	DICES	
A	SUPPLEMENTARY TABLES	54
REFERE	NCES	46

#### INTRODUCTION

When the coastal Antarctic becomes exposed to more sunlight in the austral summer, sea ice floes from the previous winter begin to melt (Stammerjohn et al. 2012; Arrigo and van Dijken 2003; Giddy et al. 2023). Coastal polynyas, characterized by open water surrounded by sea ice, form from solar heating, higher temperatures, and catabatic winds pushing the sea ice out and away from the ice shelves (Parish and Cassano 2003). The Southern Ocean is considered a high-nutrient, low-chlorophyll (HNLC) zone, with primary production limited by iron and light availability (Debeljak et al. 2023; Schine et al. 2021). The combination of increased light from open water and the iron available from winter mixing and sea ice melt enables initial phytoplankton blooms, primarily diatoms and the haptophyte *Phaeocystis antarctica* (Yager et al., 2016; Ducklow et al. 2015; Richert et al. 2019; Wang et al. 2022). Because there are no rivers and airborne dust deposition is rare in this region, additional iron from deepwater, sediments, and glacial meltwater is needed to sustain the observed bloom (St-Laurent et al. 2017; 2019). According to models, sedimentary and deep water iron likely account for a large fraction of the total Fe supply to the bloom (St-Laurent et al., 2017).

Coastal polynyas host high rates of primary productivity and carbon uptake per unit area (Tremblay and Smith 2007; Mu et al. 2014). One of the most productive polynyas is the Amundsen Sea Polynya (ASP; **Figure 1**), at a maximum net primary production of about 2.5 g C m<sup>-1</sup> d<sup>-1</sup> (Arrigo and van Dijken 2003; Arrigo et al., 2012). The ASP hosts a large phytoplankton bloom annually that starts in the southeast in November and grows towards the northwest over the next three to four months as the sea ice melts (Mu et al., 2014; Yager et al. 2016). *Phaeocystis* rapidly draws down carbon dioxide concentrations in these polynyas (Mu et al.,

2014), supplying organic matter to the rest of the polynya ecosystem, and harboring a microbial heterotrophic community (Wang et al. 2022; Richert et al. 2019) distinct from those found offshore in the Antarctic Circumpolar and the Palmer Peninsula (Delmont et al. 2014).

The dynamics between phytoplankton blooms and bacterioplankton communities in coastal polynyas are well described (Ducklow and Yager, 2007; Williams et al. 2016). Surface communities dominated by opportunistic heterotrophic bacteria actively degrade algal-derived organic matter (Teeling et al. 2012; Richert et al. 2019; Delmont et al. 2015). Some particle-associated bacteria in the surface waters likely associate mutualistically with *P. antarctica* (Delmont et al., 2014). In the mid-waters, free-living communities are distinct from particle-associated communities, with the latter more responsible for remineralizing detrital material (Delmont et al. 2014, 2015). The seasonal bloom drives changes in bacterial community structure in the surface and subsurface communities (Richert et al., 2019), but less is known about bottom-water communities and how they might change in response to sinking phytodetritus, suspended sediments, or advection by bottom currents.

In the ASP, there are three distinct water masses: Antarctic Surface Water (AASW), Winter Water (WW), and Circumpolar Deep Water (CDW) (Randall-Goodwin et al. 2015; Yager et al. 2012). Coldest WW dominates the upper water column in the winter, resulting from winter sea ice production and convection, where strong winds cause evaporation and surface waters are overturned (Kovalevsky et al., 2020). The warmer and fresher AASW forms above the WW during the spring and summer with solar heating and sea ice melt. AASW is typically characterized as freshened, warmed surface water, separated by the colder water below (Park et al., 1998; Yager et al. 2012). The warmer and saltier CDW sourced from the Antarctic Circumpolar Current off the continental shelf, is at the bottom. This deepwater contains

dissolved iron (dFe; Gerringa et al. 2012), which is likely supplemented by interacting with the nepheloid layer and sediments of the continental shelf where sediment dissolution and increased remineralization occur (Dinniman et al. 2023, 2020; St-Laurent et al. 2017). Due to a lack of full-depth convection and dense shelf water, the CDW spreads across the continental shelf and eventually reaches underneath the Getz Ice Shelf (GIS) and Dotson Ice Shelf (DIS) in the ASP (Silvano et al. 2018).

Heat from the CDW melts the underside of the ice shelf (Jenkins and Jacobs 2008). Entrained meltwater makes the CDW more buoyant so it rises from the ice-shelf cavity and flows out to the polynya, transporting CDW- and sediment-derived dissolved iron (dFe) to the upper 300 m of the water column (Sherrell et al., 2015; Randall-Goodwin et al. 2015). Sedimentary iron accounts for 39% of the total Fe supply, 75% of which is first advected into the ice-shelf cavity before delivery to the surface waters (St-Laurent et al., 2017; Dinniman et al. 2023). Glacial meltwater likely also contributes nutrients, metals, particles, and freshwater microorganisms into the now "meltwater modified" CDW (mCDW) that flows out into the polynya. The flow of iron-rich waters from the offshore CDW to the ice-shelf-outflow plume has been dubbed the "iron conveyor belt." Few studies have examined how this circulation and iron delivery affect the microbial community structure, nutrient cycling, or the rest of the food web (Alcamán-Arias et al. 2021).

A ROMS model of the ASP (St-Laurent et al., 2019) further suggests the importance of iron delivery by a coastal current (CC), which travels along the face of the ice shelves in the upper 200 m (Kim et al. 2016; Alcamán-Arias et al. 2021). This coastal current is driven by winds and is responsible for bringing freshwater and other inputs from upstream glaciers (**Figure 1**), such as the Pine Island Glacier (PIG) and Thwaites Glacier (TG; Yang et al. 2022). Both

glaciers have some of the highest basal melting rates in Antarctica; Thwaites being dubbed the "Doomsday Glacier" because of rapid ice sheet mass loss, potentially raising sea level by ~0.1 mm a<sup>-1</sup> (Scambos et al. 2017; Min et al. 2022). Little is known about how the coastal current may influence microbial communities, although model results suggest that it is a hot spot for particle deposition in the southwestern ASP (St-Laurent et al. 2019). As basal melt from the PIG, TG, and DIS continues to increase, it will likely affect both the primary production and physical properties of the ASP, influencing the microbial community as well.

Antarctic polynyas are of great interest to those studying climate-sensitive marine areas, as temperatures rise, seasonal sea ice declines and ice shelves melt at an increasing rate (Yager et al., 2012; Stammerjohn et al. 2015). The effects of freshwater input affect not only physical properties, but also primary production and the bacterial response, influencing the biological pump of carbon from the atmosphere to the deep ocean (St-Laurent et al. 2019).

This research is part of the NSF-funded *Accelerating Thwaites Ecosystem Impacts for the Southern Ocean* (ARTEMIS), an interdisciplinary effort to "bridge the gap between physics and biogeochemistry" in the Amundsen Sea Polynya. This study serves as a preliminary exploration of the diversity and potential activities of microorganisms along the "iron conveyor belt," and how they may affect the biogeochemistry of the ASP.

# The main questions of this study were:

- 1. How do bacterial communities (both free-living and particle-associated) vary by location within the ASP? By depth?
- 2. How do communities change as the CDW flows onto and across the continental shelf? Can we detect changes that reflect exchange with the sediments?

- 3. How does the bacteria community change between the CDW flowing into and the mCDW flowing out of the ice shelf cavity? Can we detect changes that indicate the contributions of the glacial cavity and meltwater?
- 4. How does the community in the coastal current change as it flows along the DIS? Is there any contribution from the basal melt of upstream ice shelves?
- 5. How do communities differ under high- and low-iron conditions? Are there any specific indicator taxa that may indicate biogeochemical processing?

#### **METHODS**

## Sample collection

Samples were collected on the R/V Nathaniel B. Palmer 22-02 expedition, (January 07– March 08, 2022) in the Amundsen Sea, Antarctica (Figure 2), and then followed a standard methodological pipeline (Figure 3). Sampling was carried out with a profiling rosette of 24 12-L Niskin bottles equipped with a SBE 911 (Sea-Bird Electronics) CTD (conductivity-temperaturedepth recorder) with additional chlorophyll a fluorescence and dissolved oxygen sensors. Water samples were collected from 3 to 6 depths at each of 21 stations and then filtered for DNA extraction. Seawater samples were collected at varying depths, including surface (ASW), intermediate (WW), and near-bottom waters (CDW; Table 1). Intermediate depths varied, but samples were collected at the temperature minimum (T-min; top of WW) or at another feature of interest such as an mCDW intrusion into the WW (Table 1). Per sample, 8–12 L of seawater were filtered first onto a 2- or 3-µm polycarbonate pre-filter (GE Water & Process Technologies), then split onto duplicate 0.2-µm Durapore (47 mm polyvinylidene fluoride membrane) or Sterivex (polyethersulfone membrane cartridge) filters (Millipore, Burlington, MA; Figure 3). A peristaltic pump at low speed and a large (293- or 142-mm) prefilter was used to avoid excessive pressure on the particle-associated cells. Communities were distinguished as "free-living" or "particle-associated" according to whether they were retained on the 0.2-µm or 2 or 3-µm pre-filter, respectively. Filters were stored in cryovials at -80C and returned to UGA within six months of sampling.

Samples for DOC concentration and composition were collected at similar stations and depths from the same conventional CTD used to collect DNA samples. Samples were frozen,

shipped home, and analyzed in the Medeiros lab (University of Georgia) using standard protocols (Letourneau and Medeiros, 2019).

Dissolved iron samples were collected at similar stations and depths (using a Trace-Metal Clean CTD that was deployed immediately after the conventional CTD) and analyzed by the Sherrell lab (Rutgers University) using standard protocols (Sherrell et al., 2015).

Nutrient samples for nitrite, nitrate, ammonia, silicate, and phosphate, were collected at similar stations and depths from the conventional CTD, filtered (0.45-µm), frozen (-80C), and analyzed at the Oceanographic Data Facility (ODF) Chemistry Laboratory at Scripps Institute of Oceanography, University of California San Diego. Silicate data were lost during analysis.

Additional samples were collected and fixed for bacterial abundance, chlorophyll *a*, particulate organic carbon, total dissolved inorganic carbon and alkalinity, and dissolved oxygen (data not reported here).

## **DNA Sample preparation**

DNA was extracted from each filter using the Zymo Research Quick-DNA Fecal/Soil Midiprep Kit according to the manufacturer's instructions (NA. cat 11-322MD).

Polymerase Chain Reactions (PCRs) were set up in a dedicated laminar-flow hood that underwent daily bleach and UV light sterilization. The V3–V4 region of 16S rRNA genes were amplified using primers 515F (GTGYCAGCMGCCGCGGTAA) and 806R (GGACTACNVGGGTWTCTAAT). Sequencing was performed on a MiSeq platform (Illumina, San Diego, CA) using 2 × 300 bp paired-end libraries according to the "16S Metagenomic Sequencing Library Preparation protocol" (Illumina). Both positive (ZymoBIOMICS<sup>TM</sup> Microbial Community Standard (Zymo Research, Irvine, CA)) and negative controls (molecular-

grade water) were included in all PCRs. The following PCR temperature cycling protocol was used for amplification of 16S rRNA gene fragments: 94°C for 3 min; 94°C for 45 s, 50°C for 60 s and 72°C for 90 s for 35 cycles; and 72°C for 10 min. PCR amplification success was evaluated with gel electrophoresis (agar 1%). Purification of PCR products was subsequently carried out using a magnetic bead purification protocol using Agencourt AMPure XP beads (Beckman Coulter, CA, USA) and following the manufacturer's protocol. All analyses were performed separately on each community, and statistical significance will not be reiterated.

#### **Sequence processing**

Reads were demultiplexed, denoised, and complied into amplicon sequence variants (ASVs) using QIIME2 v2023.7. Taxonomy was assigned using a trained naive bayes classifier from the SILVA v138 database. The ASV and taxonomy tables, metadata file, and raw sequence reads can be found at:

https://github.com/sierra-uga/ARTEMIS\_MS\_Project/tree/main/required\_files

### **Data analysis**

Samples were further distinguished according to the water mass they were collected from: either pure AASW, an AASW-WW mixture, pure WW, a WW-CDW mixture, or pure CDW according to their temperature and salinity (**Figure 4**). The endmembers of the T-S plot determined the "pure" water masses, i.e. AASW, WW, CDW, while the mixing lines between those end-members were considered "mixed" samples, i.e. AASW-WW or WW-CDW. The "pure" water masses were also determined by following the previous distributions set by Randall-Goodwin et al. 2015. Samples were also grouped by geographic location (**Figure 2**) and

by depth (0-200 m or > 200 m) and examined according to their positions along the iron conveyor belt, "CDW waterfall" (Stations 2, 4, 12, 12.3, 115, 14), inflow – outflow (Stations 14, 22, 56a, 56b; **Table 2**), and coastal current (Stations 89, 132, 106, 20, 14, 78, 56, 68, 146; **Figure 2**).

The Amplicon Sequence Variants (ASV) generated from QIIME2 were loaded into RStudio v4.4.0 using the qza\_to\_phyloseq function from the qiime2R package. The taxonomy table (Table S1), ASV table, phylogenetic tree, and metadata (Table S2) were compiled into a phyloseq object using the phyloseq R package. Before analysis, the R package decontam was used to remove potential contaminants using the prevalence and frequency method based on the controls. Using the phyloseq object, Bray-Curtis dissimilarly was calculated using the distance function in the vegan package. To compare how communities differed based on metadata groups (i.e. location or water mass), the distance matrices were run through the adonis2 function from the vegan package, which is a Permutational Multivariate Analysis of Variance (PERMANOVA) test. If output was considered significant, a multilevel pairwise posthoc test was done using the adonis.pairwise function from the pairwiseAdonis package to see which combination of groups were significant.

Canonical correspondence analysis (CCA) was carried out using the **plot\_ordination** function within the *phyloseq* package to discern the association between microbial community structure and environmental parameters. To visualize Bray-Curtis dissimilarity, nonmetric multidimensional scaling (NMDS) was also performed using the **plot\_ordination** function. To aid the visualizations and for stylistic purposes, the *ggplot2* package was used. To observe the relationships between environmental parameters without community structure, a principal components analysis (PCA) was used to explore which individual parameters corresponded

(using correlation coefficient R) with each other or with principal axes. To achieve this, the metadata was sorted based on unique station and depth and converted to a matrix, then processed and visualized with the functions **prcomp** and **plot** from base R (v4.4.0).

To test if there were certain indicator species that were in one or a combination of metadata group(s), the **multiplatt** function from the *indicspecies* package was used. Indicator species analysis was performed at the Genus level. The output was compiled into a table and visualized using Microsoft Excel v16.59.

For the differential abundance test, which attempts to find differences in the abundance of taxa between two groups (i.e. high vs low iron), an analysis of composition of microbiomes with bias correction (ANCOM-BC) was used; This was from the *ANCOMBC* package, using the **ancombc2** function. Then, the list of significant taxa names from the **ancombc2** output was used to filter the ASV table to include only those taxa. Then, the **cmultRepl** function (*zCompositions*) was used to handle count zeros and the ASV table was log-transformed. The **scale** function from base R was used to transform to z-score, to center and scale the transformed count numbers. The final transformed table was then visualized using the **Heatmap** function from *ComplexHeatmap*.

Relative abundance plots were generated to help visualize community composition. The main phyloseq object was filtered by the desired samples, then the **tax\_glom** function was used to agglomerate taxa by a specific taxonomic level. Then, taxa with a total sum of zero and low abundance taxa (<5%) were filtered out, and counts were transformed to relative abundance by the **transform\_sample\_counts** function from the *phyloseq* package. Ggplot2 and RColorBrewer were used to create the relative abundance plots. PICRUSt (Phylogenetic Investigation of Communities by Reconstruction of Unobserved States) was used to predict the functional

profiles of communities by water mass, performed on the Sapelo2 cluster from the Georgia Advanced Computing Resource Center (University of Georgia).

The **define\_water\_type** function from the *PlotSvalbard* package was used to define water masses, based on temperature and salinity, to add the water mass column to the metadata file. The map (**Figure 2**) was made using the *ggOceanMaps* function, **basemap**, to visualize the CTD casts where DNA samples were taken. The temperature-salinity (T-S) plot (**Figure 4**) from CTD casts from the ARTEMIS cruise was made using Ocean Data View (ODV).

We separated each phyloseq object into either "bloom-associated" (the upper 200 m) or "below bloom" (all depths greater than 200 m, to the seafloor). We excluded the continental slope station, Station 198, from most of the microbial community analyses since it was off the shelf and outside the polynya boundaries. We intended for it to represent an "endmember" for CDW flowing onto the shelf, but no other data confirm this to be the case. Based on velocity profiles provided by the Acoustic Doppler Current Profiler (ADCP) onboard the ARTEMIS cruise, samples were denoted "outflow" if the northward velocity was  $> 0.1 \text{ m s}^{-1}$ . Inflow stations were samples closest to the DIS, with a southward velocity  $< 0.1 \text{ m s}^{-1}$  (**Table 2**). For categorizing dissolved iron (dFe) levels, inventories  $\geq 0.5 \text{ nmol/kg}$  dFe were considered "high iron" and inventories < 0.5 nmol/kg were considered "low iron".

The bioinformatics workflow, including the PICRUSt2 pipeline, is available at https://github.com/sierra-uga/ARTEMIS-MS.

#### **RESULTS**

#### **Environmental Data**

The samples came from a full range of typical polar water temperature (-1.8 – +1.1 °C), salinity (33.49 – 34.70), and depth (2 – 1271 m) for the region, and they all represent some combination of the three main water masses (ASW, WW, CDW) with varying degrees of meltwater inclusion (**Figure 4**). Other inventories reflected the state of the bloom or biogeochemical fluxes along the iron conveyor belt (**Table S2**), with water samples exhibiting a range of nitrate (9.22–38.6  $\mu$ mol/L); phosphate (0.87–2.74  $\mu$ mol/L); nitrite (0–0.08  $\mu$ mol/L); ammonia (0.03–0.65  $\mu$ mol/L); dissolved oxygen (0.107–1.173); dissolved iron (4.17–9.36); and dissolved organic carbon (34.6–77.6). The individual metadata and nutrient profiles (**Table S2**) can also be found electronically on the GitHub provided in Methods.

In the upper 200 m, environmental parameters grouped along two principal components (PC; **Figure 5**): the first PC correlated positively with nitrate (R = 0.38), phosphate (R = 0.37), and salinity (R = 0.31) and negatively with temperature (R = -0.31) and oxygen (R = -0.37). The second PC correlated positively with latitude (R = 0.54) and depth (R = 0.50) and negatively with longitude (R = -0.48). In the waters below 200 m, the first PC correlated positively with temperature (R = 0.45), salinity (R = 0.42), and depth (R = 0.41), and negatively with oxygen (R = -0.42). The second PC correlated positively with latitude (R = 0.45) and negatively with longitude (R = -0.5). The environmental parameters in the upper 200 m grouped by water mass (**Figure 5**) and not location (**Figure 6**). Waters below 200 m were grouped by water mass and location, but not by nutrients, except for nitrite, shown by the third PC (R = -0.51); **Figure 5**, **Figure 6**).

## Free-living and particle-associated taxa and overall trends

Organisms such as *Polaribacter* (*Flavobacteriaceae*), *Pseudomonas*(*Pseudomonadaceae*), and *Nitrincolaceae* (*Oceanospirillales*), were the most abundant taxa found in both free-living and particle-associated communities across the region (**Figure 7A, 7B**; **Table S1**). Despite this result, free-living and particle-associated communities were significantly different (p < 0.001) at the Family-level (**Figure 7A, 7B**), where free-living communities included taxa like SUP05 (*Thioglobaceae*), SAR11 (Clade I/II), *Ilumatobacteraceae* (*Acidimicrobiia*), and *Nitrospina* (*Nitrospinaceae*; **Table S1**). Distinct particle-associated taxa included *Colwellia* (*Colwelliaceae*), *Pirellulaceae*, *Saprospiraceae*, and *Phycisphaeraceae* (**Table S1**).

PICRUSt analysis suggested that microbial communities exhibited the potential to assimilate many different forms of iron and used either siderophore-, ferric- or ferrous-iron uptake pathways (**Figure 8**). Most of the free-living taxa we observed shared the ability to excrete and actively uptake siderophores, while the particle-associated taxa we observed were better known for their role in nitrogen-related pathways, such as nitrification, ammonia-oxidation, or dissimilatory nitrate reduction. By contrast, particle-associated communities had a higher capacity for iron-storage pathways (**Figure 7A, 7B**). Taxa such as *Polaribacter* (*Flavobacteriaceae*), Pseudomonas (*Pseudomonadaceae*), and *Nitrincolaceae* (*Oceanospirillales*) were found most abundant in both communities, but had different distributions based on depth and location within the ASP (**Figure 7A, 7B; Table S1**).

Overall, community composition varied significantly with water mass (p < 0.001; NMDS, CCA, PCA), although some water masses harbored similar taxonomic compositions when compared pairwise. In the free-living community, the community composition in AASW

differed from that in deeper waters (WW, WW-CDW, and CDW; p = 0.01), but did not differ from the mixture of AASW-WW (p = 0.12), which was dominated by *Flavobactericeae* and *Oceanospiralles*. Deeper free-living communities in WW and CDW were different from all other water masses or mixtures (p = 0.01). In the particle-associated communities, the AASW composition did not differ from that of the WW (p = 0.28), but they were distinguishable from the WW-CDW and CDW communities (p = 0.01). The WW and CDW communities also contained different particle-associated taxa, including *Pseudomonas* or *Colwellia* (p = 0.01).

### Community structure in upper 200 m

The upper 200 m included AASW, WW, and some mixture of WW-CDW, which may be mCDW from underneath the Dotson Ice Shelf getting upwelled and then entrained into the coastal current. Free-living and particle-associated community structure only differed significantly at open polynya from Dotson Ice Shelf stations (p = 0.01). The lack of significant difference for the other locations may be due to small sample size, which influences Type II error. For instance, the Getz group only had two CTD casts, while open polynya had five. CCA was used in conjunction with environmental factors to compare regions in the ASP. In the free-living CCA (**Figure 9A**), the top two axes accounted for 23.9% of variance and taxonomic information, with oxygen and nitrate demonstrating the highest explanatory power, denoted by the length of the environmental vector arrow. In the particle-associated surface CCA, the top two axes accounted for 34.5% taxonomic variance, with nitrate and nitrite as the most explanatory power.

In the upper 200 m, both free-living and particle-associated communities were dominated by bloom-associated taxa such as *Polaribacter (Flavorbactercae)* and *Oceanospirillales*, no

matter location (**Figure 7A, 7B**). In the indicator analysis (**Table 3**; **Table 4**), confirmed by the CCA (**Figure 9A, 9B**), no specific species appeared as indicators based on location in the surface waters of the polynya. At Station 174, part of western open polynya (**Figure 2**), the particle-associated taxa were distinctly different from other stations, especially in the surface, due to the high prevalence of *Saprospiraceae* (**Figure 9B** and **Figure 7A, 7B**). Only one free-living organism, an unidentified *Flavobactercae*, was found to be an indicator for Getz Ice Shelf stations (p = 0.04; **Table 3**).

### Community structure below 200 m

Community structure in deep water (> 200 m; WW, WW-CDW, and CDW; **Figure 10C**, **10D**) varied with location within the polynya, based on PERMANOVA and the CCAs of deeper waters (p = 0.02; **Figure 10C**, **10D**). In the CCA of free-living samples (**Figure 10C**, **10D**), the first two axes accounted for 27.3% of variance, with oxygen and temperature demonstrating the highest explanatory power. In the CCA of particle-associated surface samples, the first two axes accounted for 27.5% taxonomic variance, with the highest power from ammonia.

In free-living communities, SUP05 (*Thioglobaceae*; a sulfur-oxidizing bacteria) and *Nitrosopumilus* (*Nitrosopumilaceae*; an ammonia-oxidizing archaea) dominated WW to CDW (**Figure 7A, 7B**; **Figure 11**). *Nitrosopumilus* was found uniformly in deep-water free-living samples, despite location, where nitrate was high, and ammonia was low. For simplicity, archaeal analysis was excluded from the other analyses in this study, but re-running PERMANOVA with Archaea showed that communities, based on location and water mass, were still different (**Figure 11**). Certain deepwater particle-associated taxa, like *Pseudomonas* and *Porticoccaceae*, were found consistently in WW and CDW samples (**Figure 7A, 7B**; **Table S1**).

The structure of both free-living and particle-associated deepwater communities was driven partially by their location in the ASP, which may be a result of nutrient availability or proximity to bloom (p = 0.02) as it grew from the southeast to the northwest during the summer. Free-living communities exhibited many indicator taxa at the Dotson, eastern CC, and Getz stations, including *Woesia* (p = 0.12), *Nitrospina* (p = 0.03), and Sva0996 (p = 0.02; **Table 4**). *Saccharospirillaceae* was an indicator species for free-living communities in the open polynya (**Table 3**). Particle-associated communities in deeper waters did not have as many indicator taxa, but Pseudomonas was also found in the Dotson, eastern CC, and Getz station cluster (**Table 3**).

#### **CDW** inflow to ASP from continental shelf

As the CDW from the circumpolar current travelled down the retrograde continental shelf toward the ice shelves, there was a change in community structure. Stations 2 and 4, both open polynya stations nearer to the shelf break, harbored a higher relative abundance of *Pseudoalteromonas* (*Pseudoalteromonadaceae*) and *Vibrio* (*Vibrionaceae*), unique to these two stations. *Pseudoaltermonas* dominated the near-bottom community at Station 4 (**Figure 12**). As the communities reached closer proximity to the Dotson Ice Shelf, they began to resemble other deepwater communities at the shelf, with organisms like SUP05 and SAR11. Along with this change, sea-ice related species like *Colwellia* began to increase in abundance closer to the Dotson (**Figure 7A, 7B**).

#### Inflow, DIS outflow, and coastal current

A central objective of this study was to determine if the bacterial community changed during the passage of CDW through the ice-shelf cavity and its entrainment of basal or subglacial meltwater. We found that free-living and particle-associated communities in the

outflow plume were significantly different from the inflow (p = 0.02, 0.03, respectively), but the indicator analysis showed that much of the distinction between free-living and particle-associated communities came from taxa found in the inflow but not in the outflow. This finding suggested that particle-associated taxa were generally lost but not gained during the passage. In contrast, the free-living community in the outflow exhibited seven indicator taxa (**Table 5**), including *Colwellia*, that distinguished the outflow from the inflow. A differential abundance analysis, ANCOM-BC, similarly identified different free-living taxa, like *Pseudomonas* and *Rhodobacteraceae*, in the outflow versus the inflow (**Figure 13**; **Table S1**). It is likely that the indicator species analysis identified low-abundance (rare) taxa, which could correspond to the relatively low input (1-2%) of glacial meltwater to the mCDW. The community of the inflow (Station 14) versus the outflow (Station 56a, Station 56b, and Station 22; **Figure 2**) showed very similar family-level structure in the relative abundance plots (**Figure 7A, 7B**)

As the outflow began to mix into the coastal current (CC) and shoal into the open polynya, the communities showed changes as the current traveled north and westward. Based on the indicator analysis and relative abundance plot (**Figure 7A**), the CC communities were likely influenced by bloom dynamics because of the increased presence of bloom-related taxa, such as *Flavobacteriaceae* and *Nitrincolaceae*. It is worth noting that eastern CC and western CC communities were quite different in both free-living and particle associated taxa (p = 0.001). *Nitrospina*, an important nitrite-oxidizer, was found in the indicator analysis for Eastern CC, namely at Station 89, where surface phytoplankton abundance was very low and surface iron concentration was considerably higher compared to the open polynya (**Figure 7A, 7B**; **Figure 12**; **Table S2**). The surface waters at this station were likely recently exposed meltwater inputs from the Thwaites and Pine Island glaciers.

## High and low iron communities

Within both free-living and particle-associated communities, taxa were significantly different (p < 0.001) for high- versus low-iron samples and they could be distinguished using both indicator species and differential abundance analysis. Using ANCOM-BC, free-living taxa such as *Nitrospina*, *Roseibacillus*, and *Ilumatobacteraceae* were enriched in high-iron samples (**Figure 14**). Similarly, specific taxa such as *Salinirepens*, *Pseudomonas*, and *Pirellutaceae* were found in high-iron particle-associated communities (**Figure 15**). As noted above, *Pseudoalteromonas* and *Vibrionaceae* were present in both size fractions from CDW samples in the northern Dotson Trough (Station 2 and Station 4), where dissolved iron was low (<0.5; **Figure 7A, 7B; Figure 12**).

#### DISCUSSION

The aim of this study was to explore whether specific bacterial taxa could be responsible for processing iron from known sources along the iron conveyor belt, such as glacial melt, sediments, or CDW. Our results suggest that distinct communities within the ASP – such as the communities at the bottom of the Dotson Trough, or the Dotson outflow and western polynya.

Due to the inherent limitations of 16S rRNA metabarcoding approaches, it was difficult to recognize specific iron-processing taxa, particularly in remote regions like Antarctica, where many microorganisms are uncultured and understudied. The potential for iron-processing was only assessed through predictions of genome function using PICRUST2 and was not investigated directly through metagenomic or metatranscriptomic sequencing. Considering this, we focused on documenting the dominant organisms within this system, which correlated with depth, the proximity to CDW, glacial outflow, or the *Phaeocystis* bloom itself.

Our findings from the polynya surface and intermediate waters agree with previous microbial community studies within the ASP. For instance, Delmont et al. (2014) show a distinct free-living and particle-associated community, which corresponds considerably to the *P. antarctica* bloom. Additionally, Richert et al. 2017 found that bacterial communities were distinct with depth, precisely the different water masses: AASW, WW, and CDW, with surface communities dominated by heterotrophic bacteria also found in Delmont et al. 2014. Our results for the open polynya region are similar, with surface waters consisting of opportunistic organic degraders such as *Polaribacter* (*Flavobacteriales*), SAR92 clade (*Porticoccaceae*), and *Nitrincolaceae* (*Oceanospirillales*), which are known to be associated with *P. antarctica* blooms (Choi et al. 2016; Delmont et al. 2014; Piontek et al. 2022; Delmont et al. 2015; Thiele et al.

2023). Those studies report that the surface communities are less diverse than bottom waters, which is also consistent with our results. It is worth noting that *Nitrincolaceae* has been associated with late summer bacterial communities in the ASP, and many taxa discussed in this study have been found to differ in their translational regulation based on season in the Southern Ocean (Debeljak et al., 2023).

This research had an opportunity to examine the deep waters more thoroughly than before, especially those nearest to the ice shelf cavities. Deeper in the water column, the freeliving and particle-associated communities are more distinct. Compared to the surface, where similar organisms dominate in both types of communities due to the presence of *Phaeocystis*, the bottom waters harbor unique organisms. In particle-associated communities, *Pseudomonas* (Pseudomonadaceae) dominates most of WW to CDW, besides the AASW-WW toward the Eastern notch. This prevalence is likely from the input of basal melt from the upstream glaciers (PIG and TG), where we found that *Pseudomonas* dominates near high iron sources and appeared in Dotson glacial outflow (Silvano et al. 2018). Pseudomonas species are known to have very diverse genomic capabilities, including production of extracellular polymeric substances (EPS), carrying out nitrogen fixation, denitrification, and degrading hydrocarbons. This bacterial group has been found in high nitrate environments, such as wastewater, which corresponds with the nutrient gradient in the ASP, with higher nitrate at depth (A. Choi et al., 2016; Arat et al., 2015; Nilsson et al., 1980) In open polynya samples of pure CDW, the particleassociated communities included Colwellia, a known sea-ice related organism that produces EPS to retain salt and reduce freezing; along with this, it can use nitrate as an electron acceptor, perhaps contributing to the denitrification process of turning NO<sub>3</sub><sup>-</sup> to N<sub>2</sub> (Thiele et al. 2022). Dominant taxa in deeper waters below the bloom included Archaea, Nitrosopumilus (an

ammonia-oxidizer), and SUP05 (a sulfur-oxidizer). *Nitrosopumilus* and ammonia oxidation are important to high-latitude areas, including ASP, supporting the nitrogen cycle, and potentially iron cycling (Thiele et al. 2023; Anantharaman et al. 2013; Gwak et al. 2023).

In other areas of West Antarctica, such as the Ross Sea, a previously published transcriptomic analysis confirms that sulfur-oxidation and nitrification occur underneath ice shelves, where ammonia from the basal melt is high (Martínez-Pérez et al. 2022; Anantharaman et al. 2013). We seem to find similar communities in the ASP, though we do not detect Nitrospina (Nitrospinaceae), a nitrite-oxidizing bacteria that usually accompanies Nitrosopumilus to complete the nitrification pathway. Nitrospina was found where surface iron was higher in concentration, possibly from upstream glacier influence. The missing nitrite oxidizer in the rest of the polynya may come from a different genus, such as Nitrincolaceae or Pseudomonas, which is difficult to speculate without transcriptional analysis. Nitrosopumilus, found only in deeper waters, is also known to perform dark carbon fixation, taking in CO<sub>2</sub>, and converting it into organic carbon, which may be an unexplored carbon supply to the polynya (Kharbush et al. 2020; Martínez-Pérez et al. 2022). This result may also be supported by the increase in DOC in the Dotson outflow, incorporated into the Western CC. This has been found mainly under ice shelves, but Nitrosopumilus and SUP05 at the face of the DIS and GIS may indicate a similar function (Martínez-Pérez et al. 2022; Lopez and Hansell 2023; Min et al. 2022). SUP05 is known to exist in oxygen minimum zones and has been found in other areas of the Antarctic, at the Western Antarctica Peninsula (WAP) or the Ross Sea (Anantharaman et al. 2013; Morris and Spietz 2022; Liu et al. 2024).

This consortium we found of S-oxidizing lithoautotrophs and nitfrying organisms may be key component to iron cycling in the ASP, answering one of the original aims of ARTEMIS. A

recent GEOTRACES special issue that discusses nitrogen availability and its overall cycling in the ocean, reports that the nitrogen cycle is largely mediated by enzymes that require trace metals, such as iron, as catalysts (Casciotti et al. 2024). Nitrification, denitrification, nitrogen assimilation, and anammox all require Fe and other trace elements to occur. The waters where these processes occur, such as underneath ice shelves, where iron is high, may be advected back to the polynya. Higher iron concentrations stimulate higher rates of nitrification, and this correlation may provide new bioavailable iron (Hogle et al. 2016; Ma et al. 2021). Though we found just a few indicator species in the Dotson outflow, many organisms were lost from deep CDW inflow, perhaps indicating a dominant heterotrophic organism within the cavity. This result would agree with results from under the Ross Sea Ice Shelf (Martínez-Pérez et al. 2022). However, confirmation of this hypothesis would require a direct bacterial abundance measurement. Those analyses are forthcoming from the ARTEMIS grant. Such an increase in heterotrophic activity may release bioavailable iron back to the polynya.

Iron is a significant determiner of the biological activity in this HNLC zone. While CDW and sediment resuspensions are primary iron sources, glacial and sea-ice melts also stimulate production. As stated before, as planetary warming increases, so will ice shelf melt as warmer waters can intrude into the cavities more quickly (Silvano et al. 2018). With the evidence of the importance of bacterial communities to many nutrient cycles in this area, it is essential to understand any microorganisms that may play a role in iron cycling, especially as more iron is released into the polynya. When comparing high and low iron communities, we could not infer any specific iron-reducers or iron-oxidizers based on taxa alone. However, many organisms were correlated with higher iron concentrations. For free-living communities, we identified organisms such as the NS5 marine group, a known aerobic heterotrophic organism with nitrogen and

phosphorous metabolism, which was only found in stations near ice shelves (Priest et al. 2022). We also found *Rhodopirellula*, another aerobic chemoorganotrophic bacteria associated with global carbon and nitrogen cycles (Žure et al. 2017). For particle-associated taxa, *Pseudomonas* was enriched across all samples, with especially high relative abundances in the high iron samples. As previously stated, *Pseudomonas* is typically found in high-nutrient conditions and has diverse genomic capabilities, further supporting the coupling of nitrogen, carbon, and iron cycling in this area. In the particle-associated taxa, we also identified other organisms, including *Salinirepens*, *Gimesiaceae*, and *Pirellulaceae*, which are ubiquitous heterotrophic bacteria (Bowman 2014; Cho et al. 2020). It is likely that iron and nitrogen co-vary in this environment, due to the many nitrogen-related organisms upregulated in high iron samples.

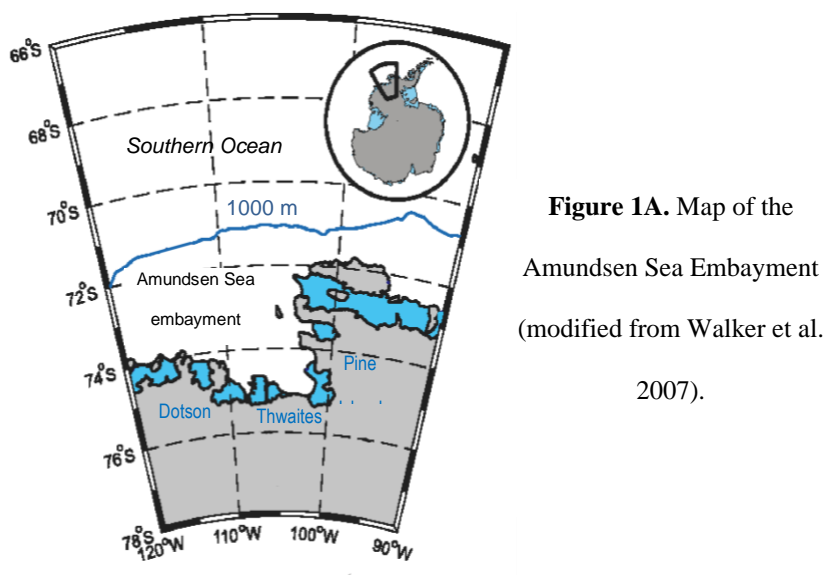
Though we did not identify any specific iron-related taxa, it may be a matter of the limitations of the 16S rRNA metabarcoding approach, the lack of biological and technical replicates, or the lack of cultured organisms in this system. Many factors could affect the detection of iron-related taxa, such as time, location, and proximity to bloom. The supply of organic matter ultimately determines the composition of benthic microbial communities (Richert et al. 2017). *Pseudoaltermonas* and *Vibironaceae* were found in open polynya CDW samples, where iron was low, and both genera are known to be able to produce siderophores and synthesize vitamin B12, which can help stimulate phytoplankton growth (Bertrand et al. 2007, Santiago et al. 2024). These organisms may take up iron and bind them to organic molecules, which is typically part of dFe concentrations (J. Park et al. 2023; Bundy et al. 2018). It may be the case that they are outcompeting other microorganisms by decreasing the amount of available iron to other microbes (J. Park et al. 2023). Though not a perfect method, PICRUSt2 can be used to determine the potential genomic capabilities of Antarctic microbial communities. We found

that all communities are uniformly equipped with iron-related genes, with siderophore uptake being a potentially prominent genomic pathway in free-living communities. As many organisms in this dataset are uncultured and understudied (and genomic predictions rely on public databases of bacterial genomes), PICRUSt only serves as an estimate for what organisms may be capable of expressing.

#### CONCLUSION

This study offers a first glimpse into the bacterial communities along the iron conveyor belt and their potential role in biogeochemical cycling in the ASP. In summary, our research suggests that inflow and outflow communities were not significantly different at the DIS but change towards the west. Also, nitrification may be a key player in both nitrogen and iron cycling, basal melt from upstream glaciers likely influences the coastal current and community composition, and there may be siderophore-producing organisms in CDW below the open polynya. While we initially anticipated an iron-centric narrative, our findings unveiled greater complexity that demands further investigation for comprehensive understanding. A future study incorporating metagenomics, transcriptomics and experimental manipulation could bridge the knowledge gaps identified in this project. As sea-surface temperatures continue to rise and stimulate glacial melt – adding additional iron to the system, reducing sea ice formation, and reducing the formation of bottom water, it becomes increasingly crucial to comprehend how this environment and its microorganisms may change in the future. Such understanding can enhance our projections, enrich our knowledge of global cycling and circulation, and bolster the protection of these systems.

# **FIGURES**



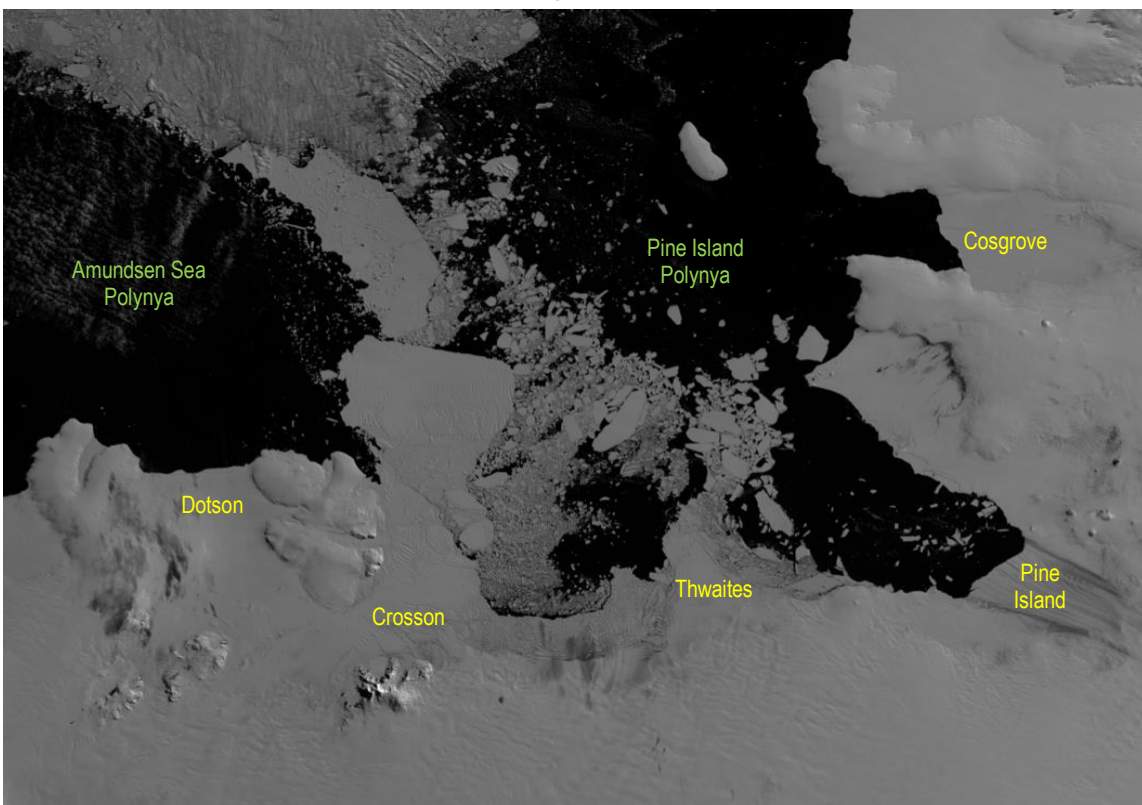


**Figure 1B.** MODIS satellite image (*nsidc.org/data/iceshelves\_images*) from Feb 2019 of southeastern Amundsen Sea with its two notable polynyas labeled in green and five rapidly melting ice shelves labeled in yellow.

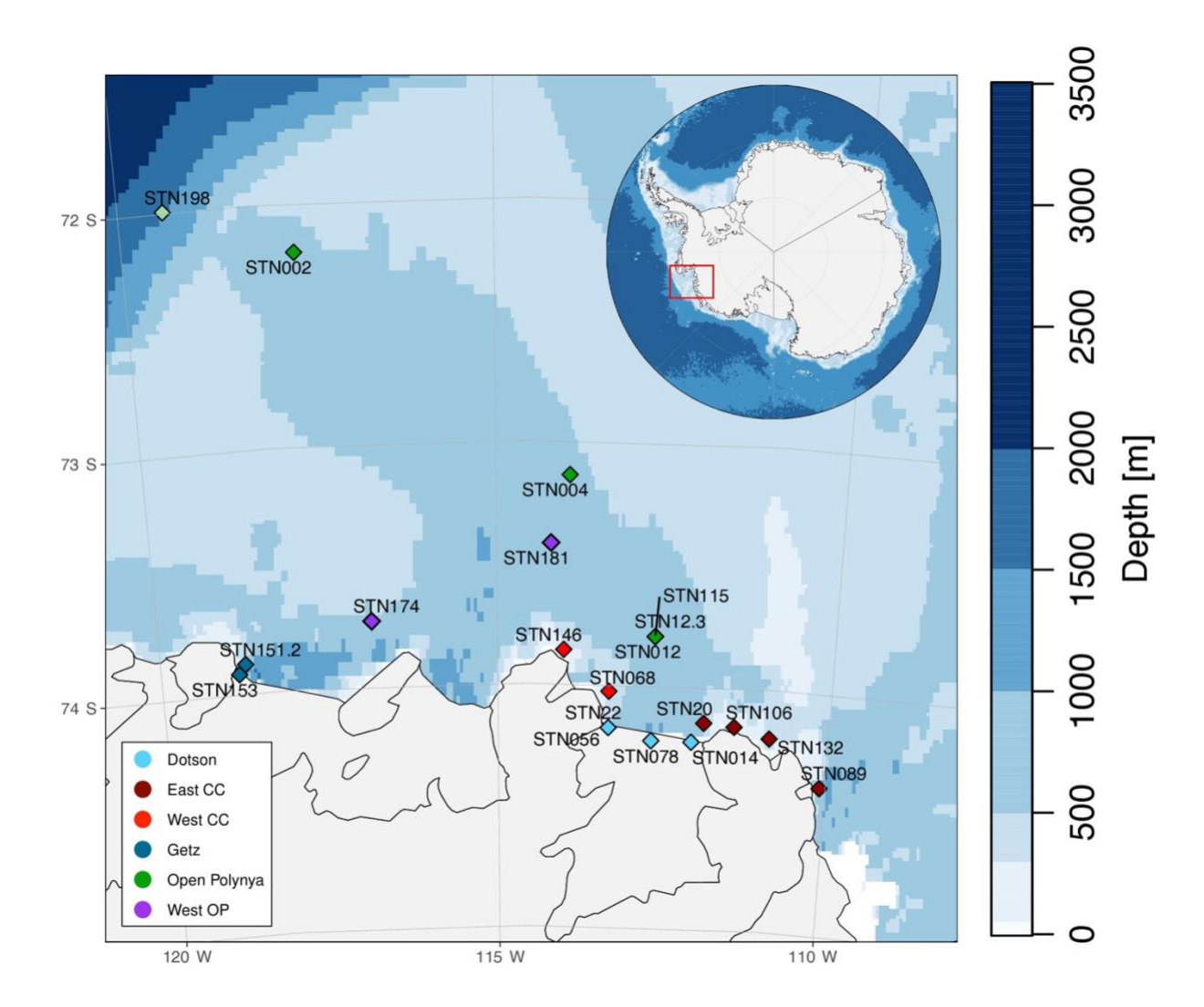
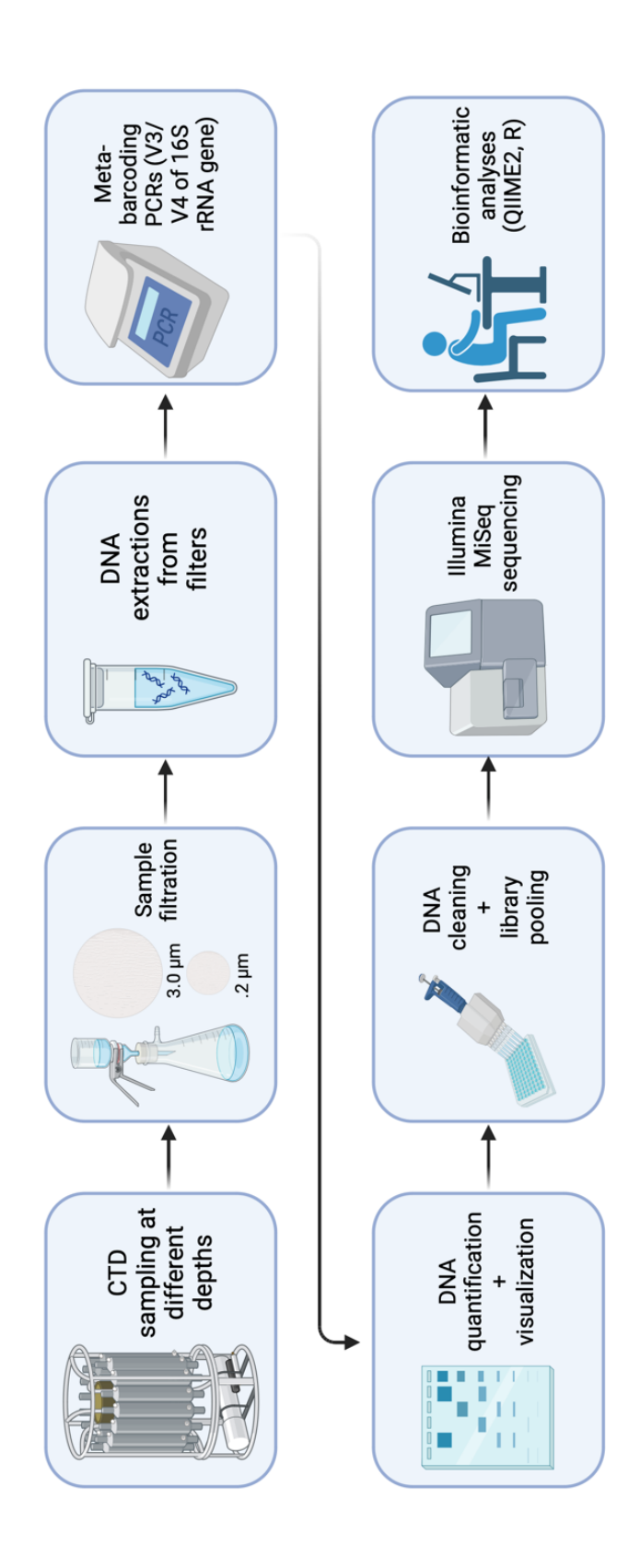
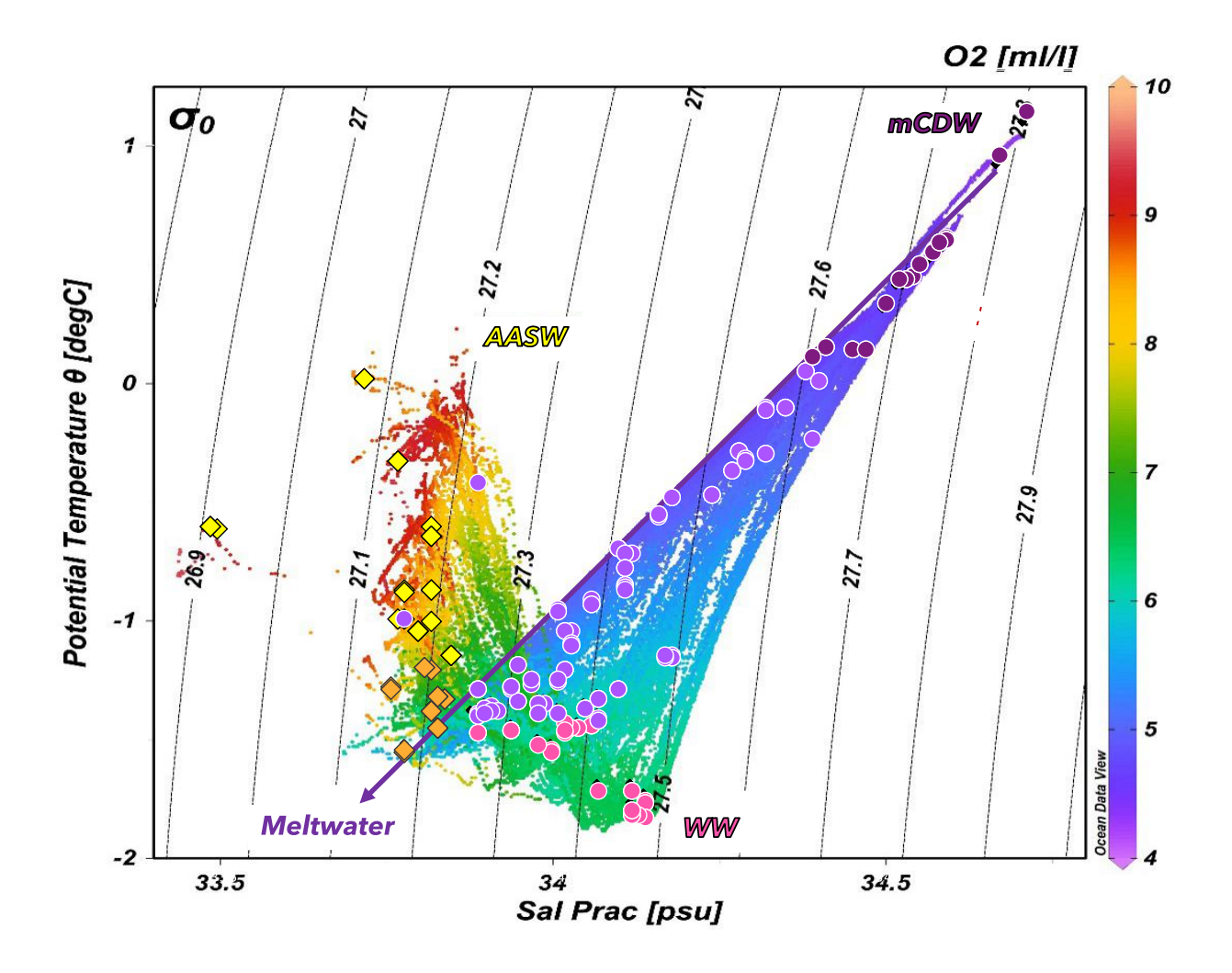


Figure 2. Station map with bathymetry. Colors are coordinated with location.

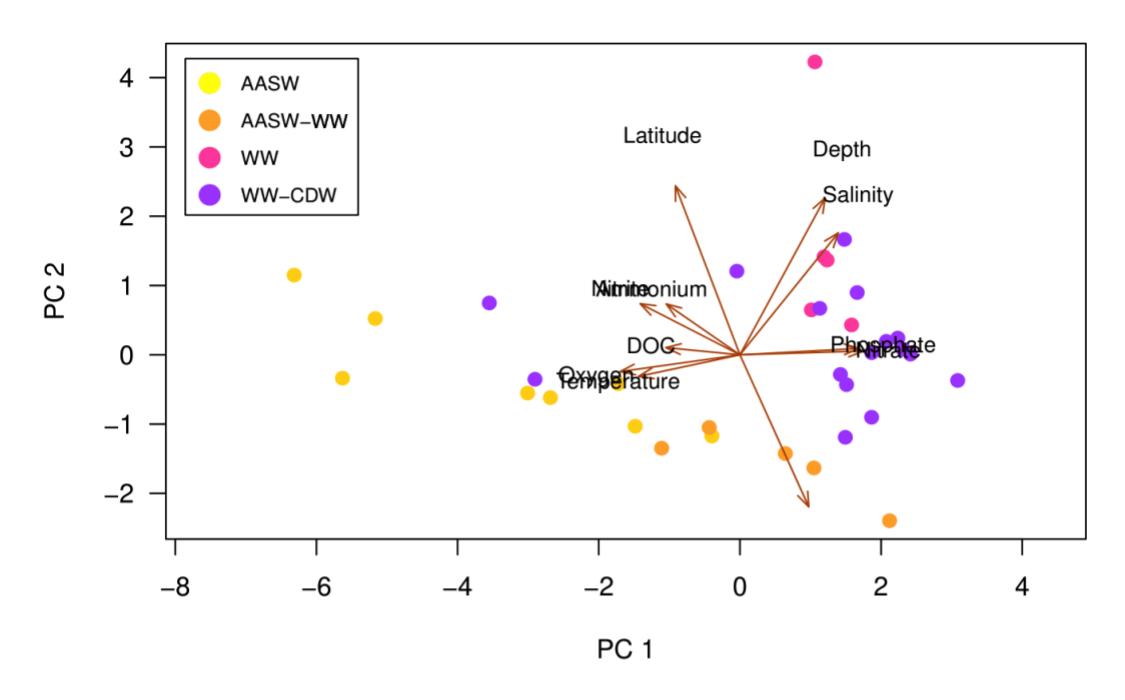


**Figure 3.** Pipeline of study.



**Figure 4.** Temperature-Salinity plot for all ARTEMIS CTD casts, with oxygen as color and black points as samples with DNA collected.

# Upper 200m



### Below 200m

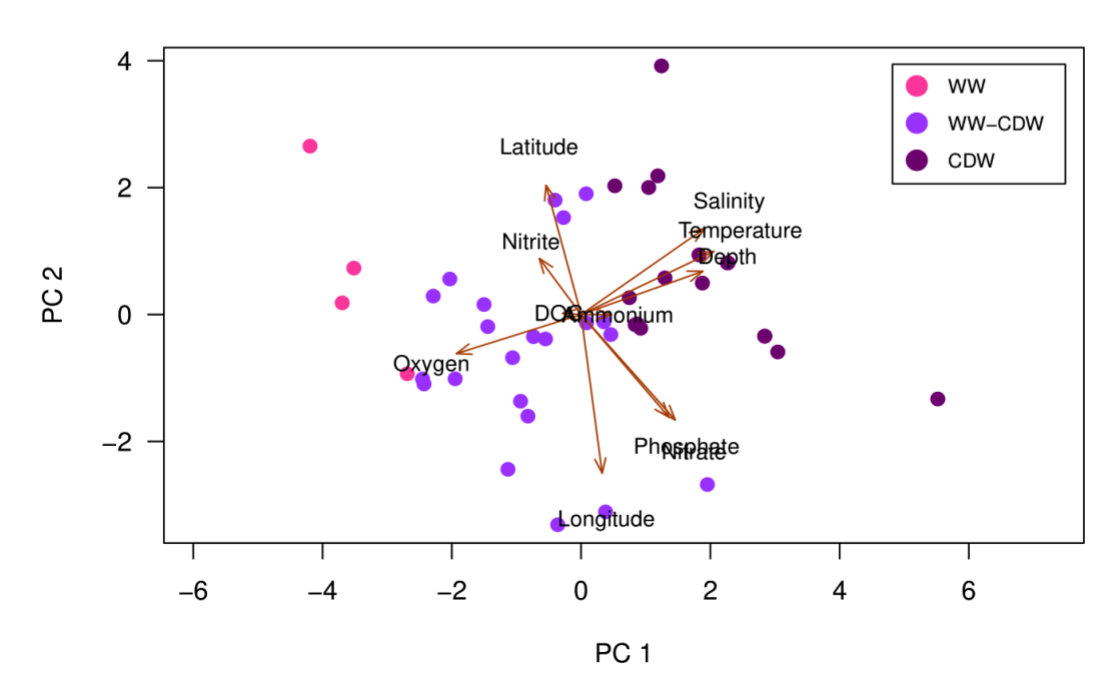
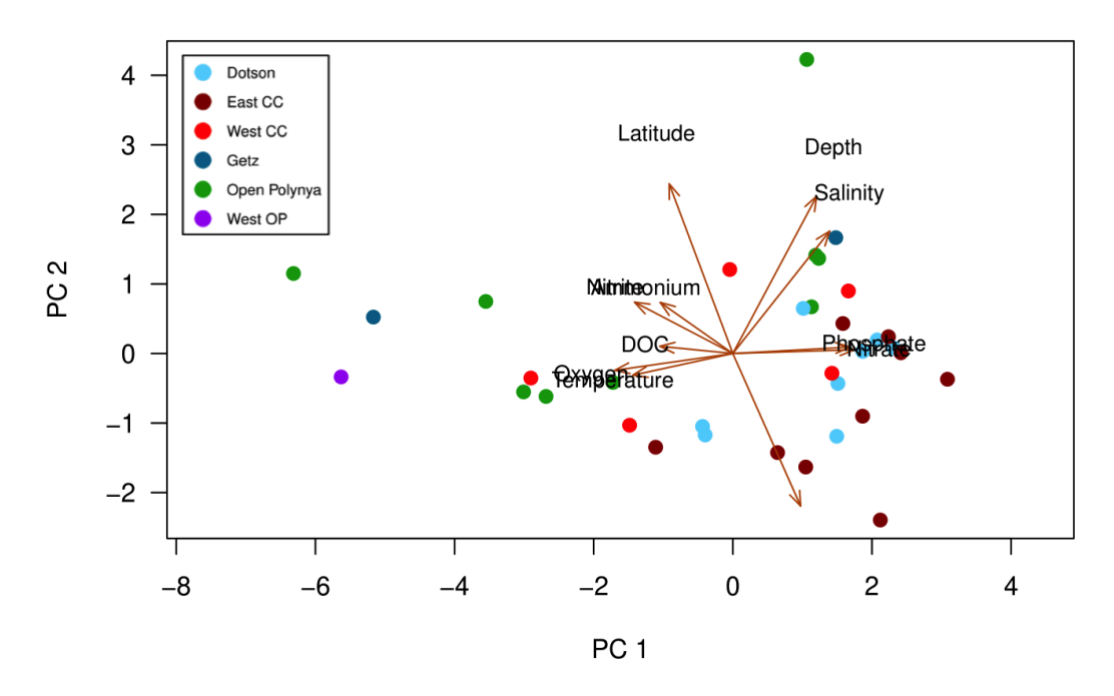
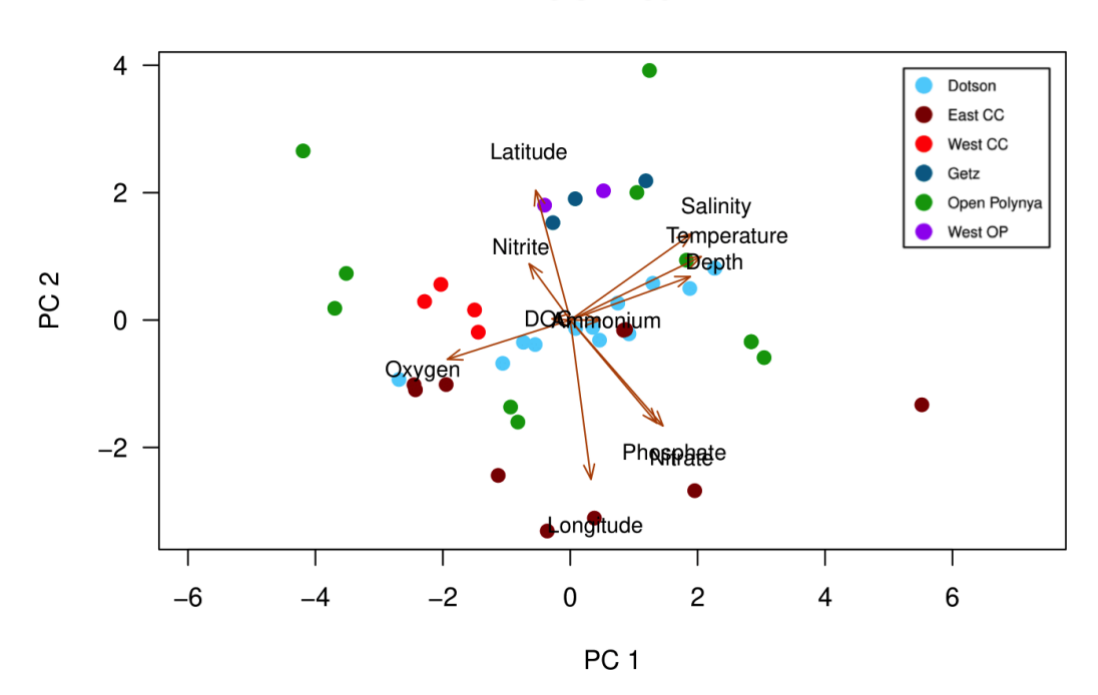


**Figure 5**. PCA of sample metadata by water mass in the ASP. Top PCA is surface-200m and bottom PCA is 200 m to seafloor.

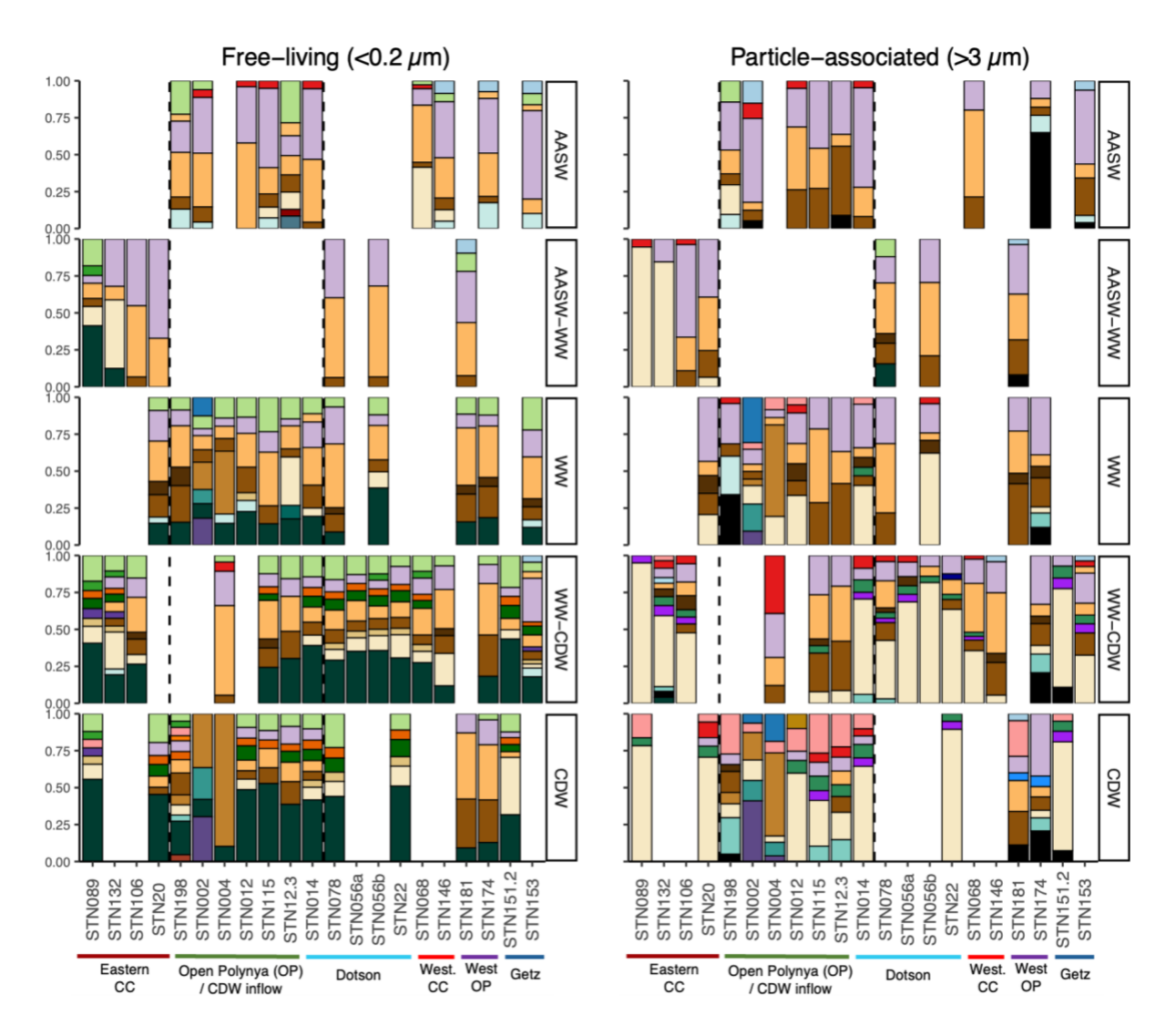
## Upper 200m



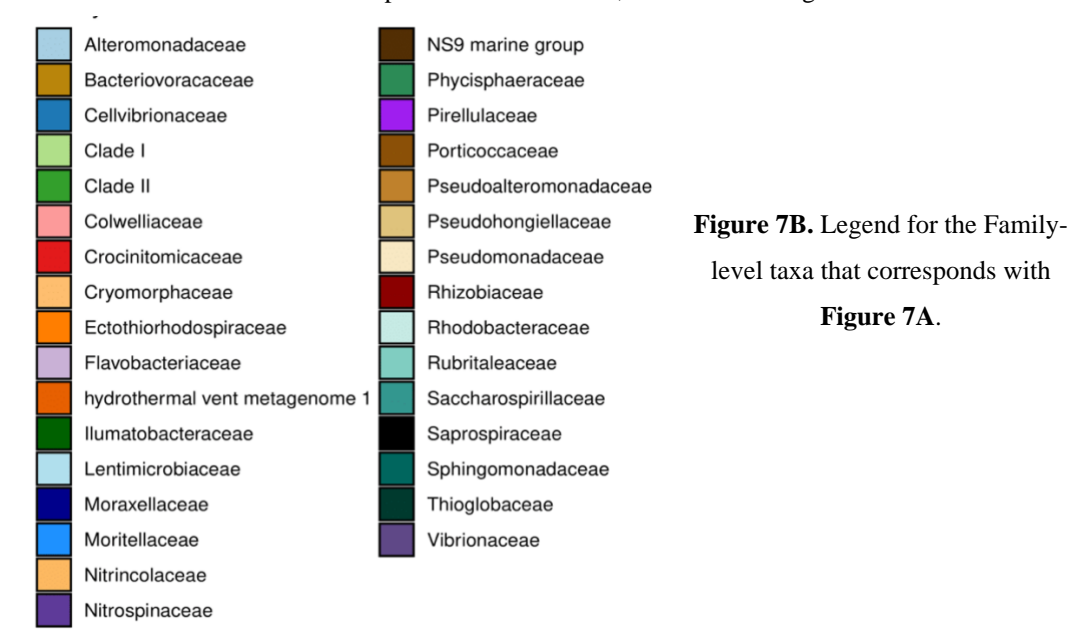
#### Below 200m

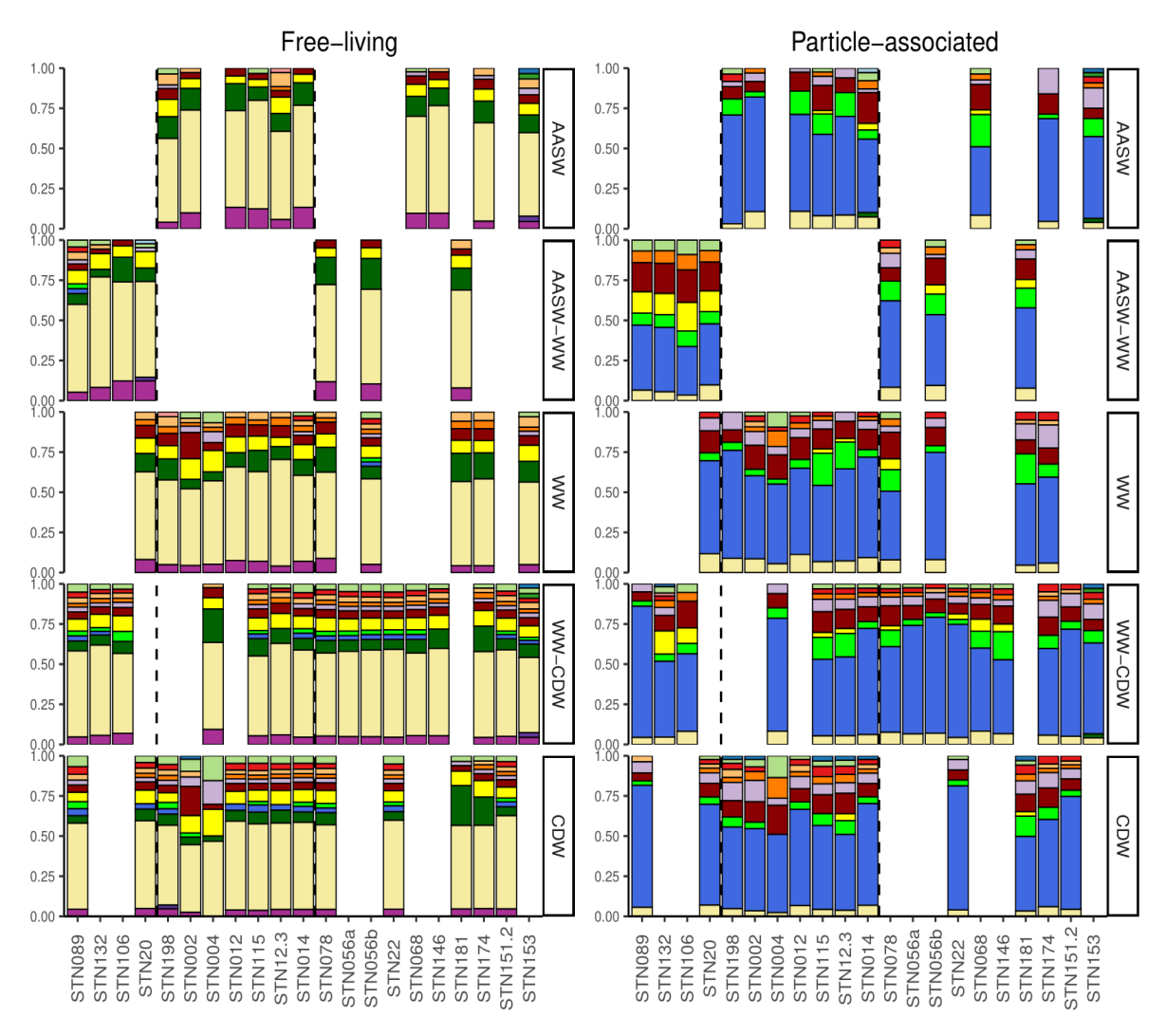


**Figure 6.** PCA of sample metadata by location in the ASP. Top PCA is surface-200m and bottom PCA is 200-bottom.

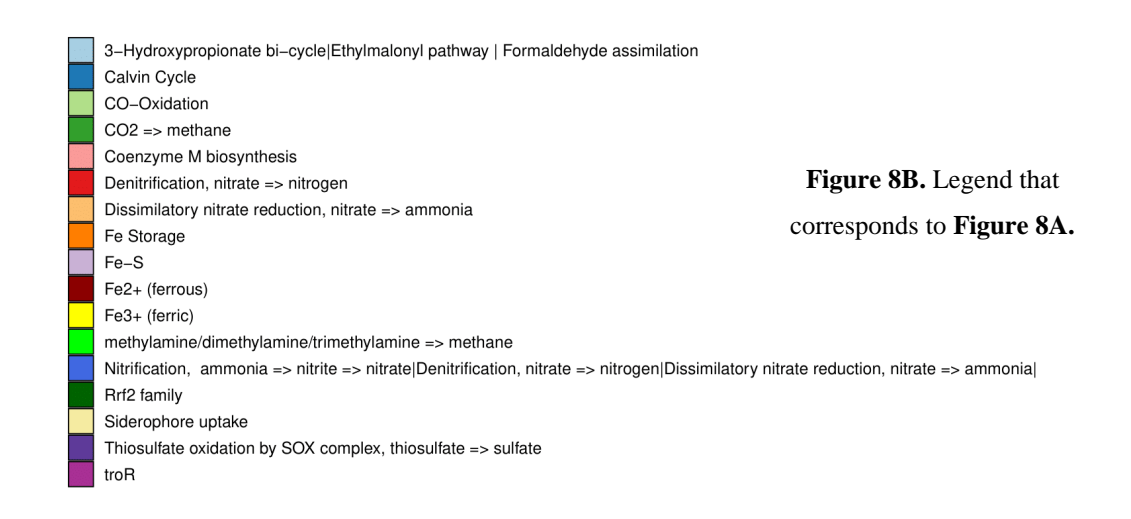


**Figure 7A.** Relative abundance for free-living (left) and particle-associated (right) communities at the family level. Each row represents a water mass, labeled on the right.





**Figure 8A**. Relative abundance of PICRUSt2 KO numbers by water mass and station. Free-living on left and particle-associated on the right.



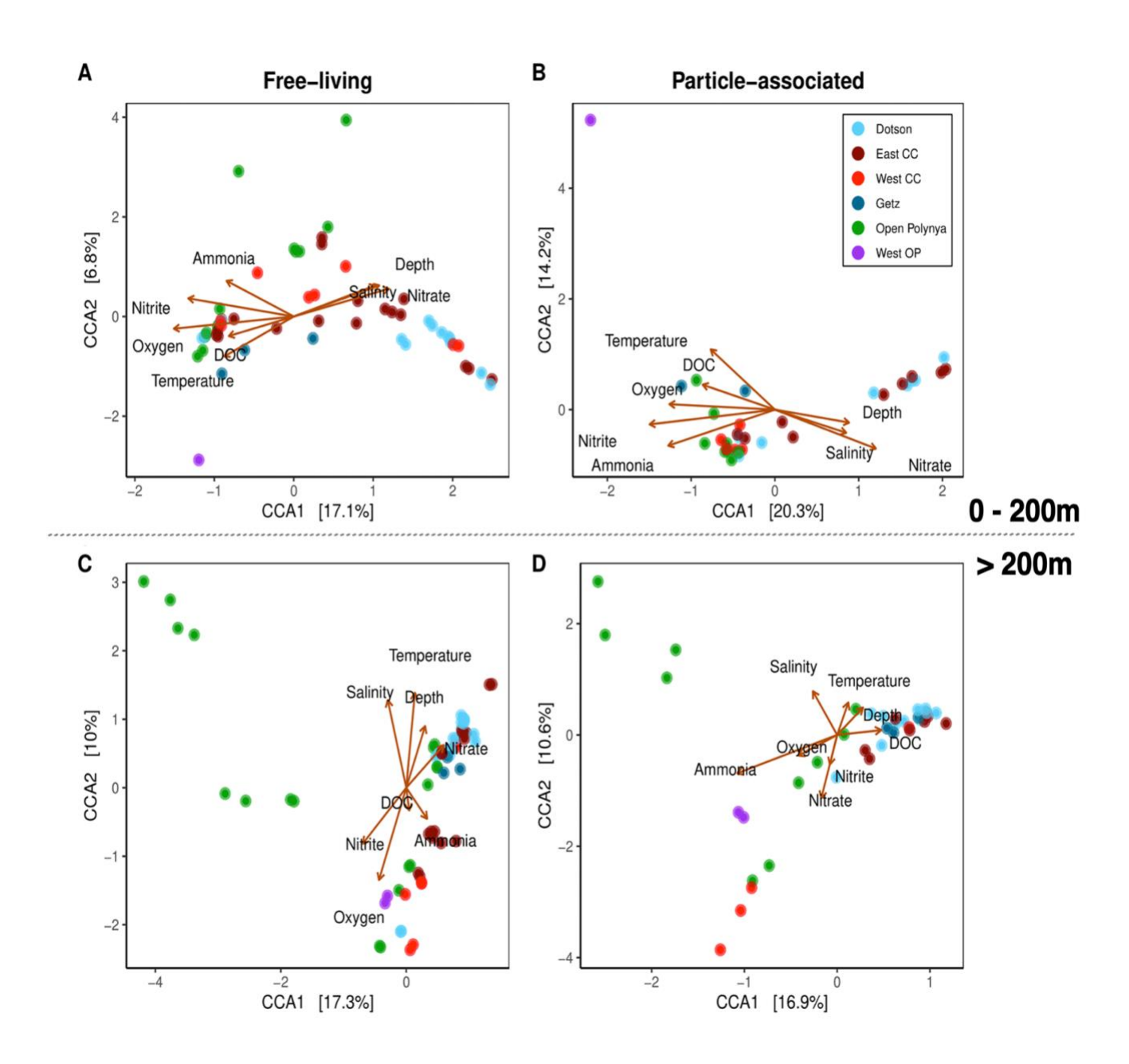


**Figure 9.** Canonical Correspondence Analysis (CCA) of free-living (**A**, **C**) and particle-associated (**B**, **D**) bacterial communities based on **location** within the ASP. First row CCAs are surface-200m and bottom row CCAs are 200m-bottom.

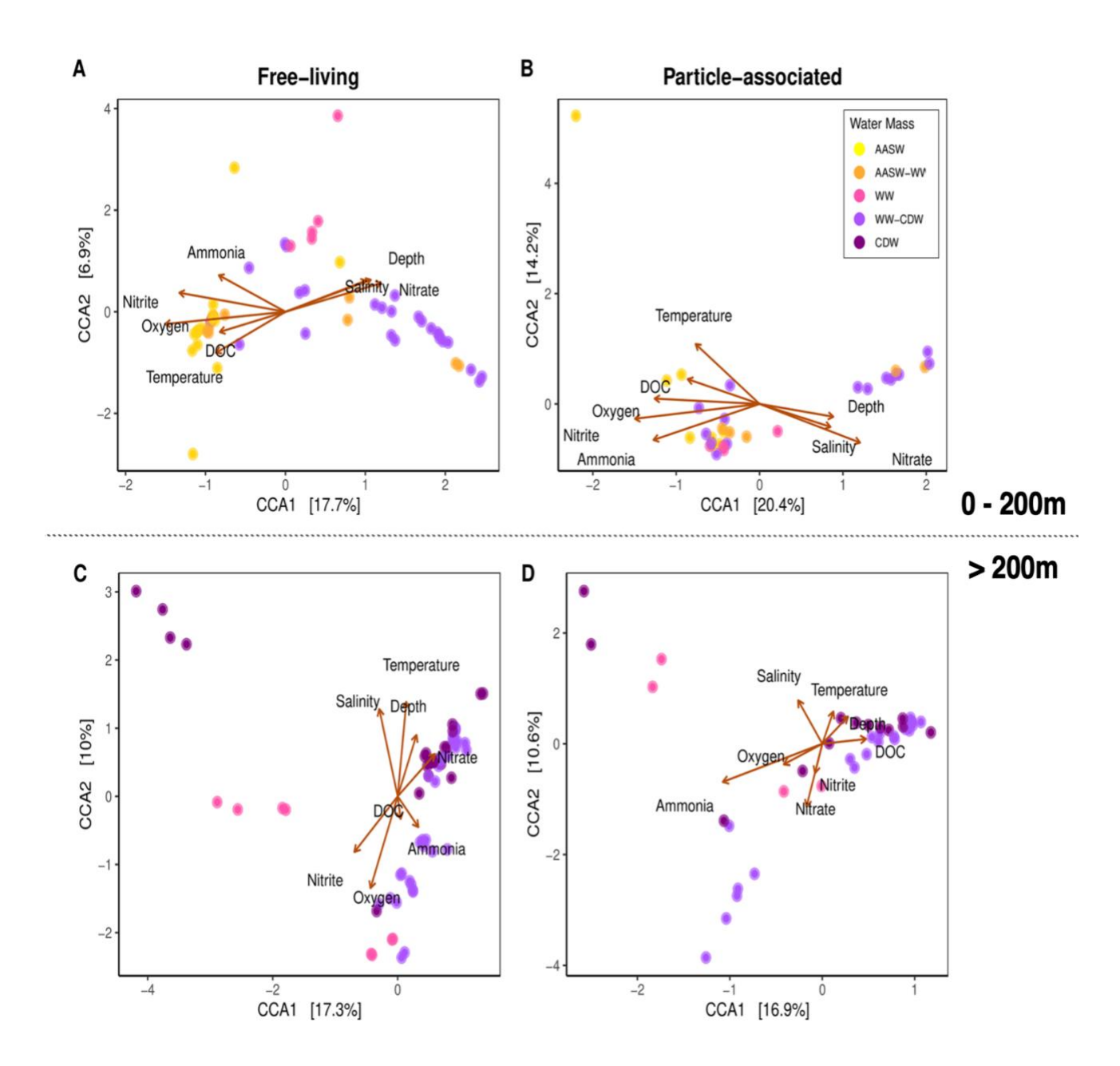
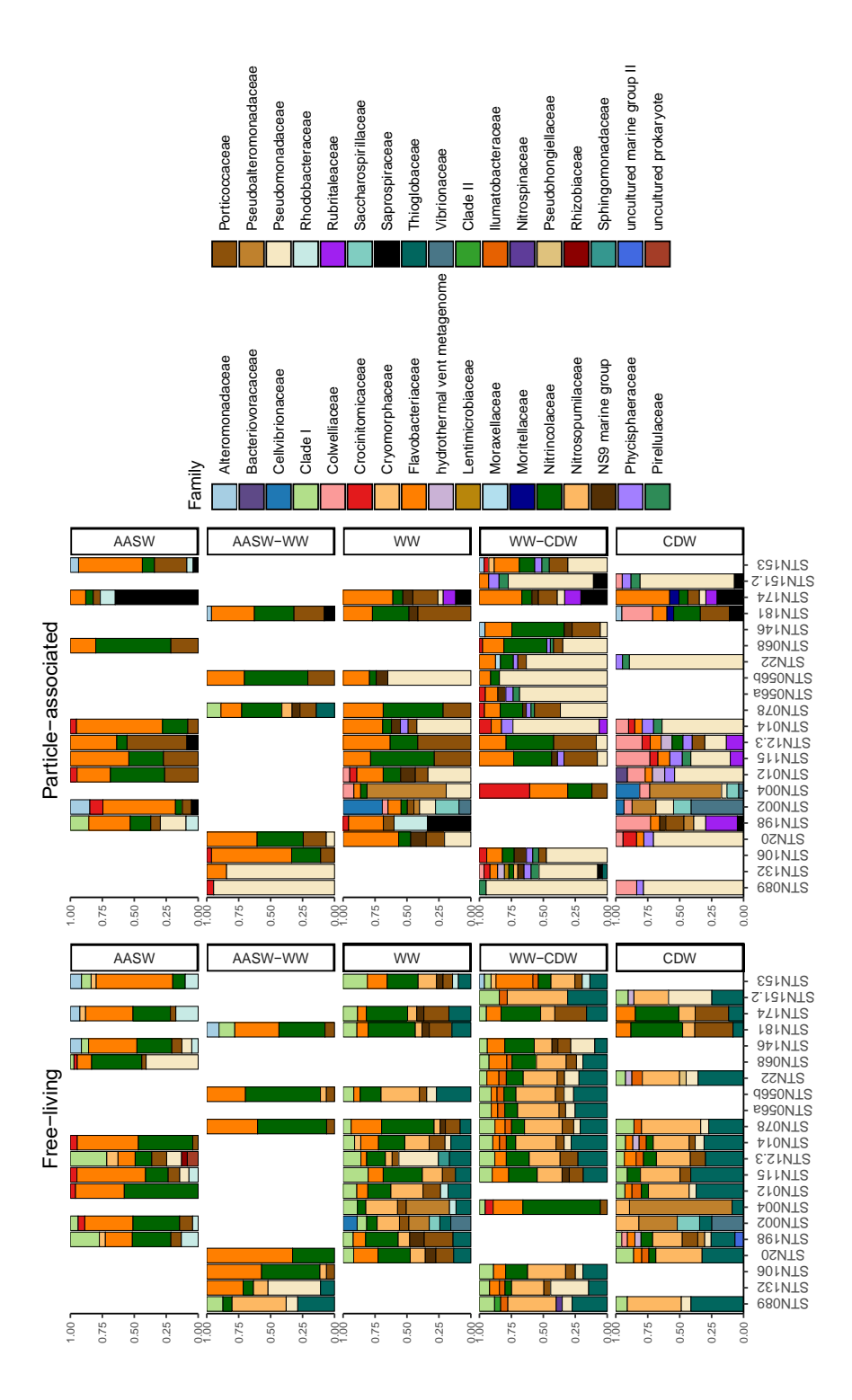
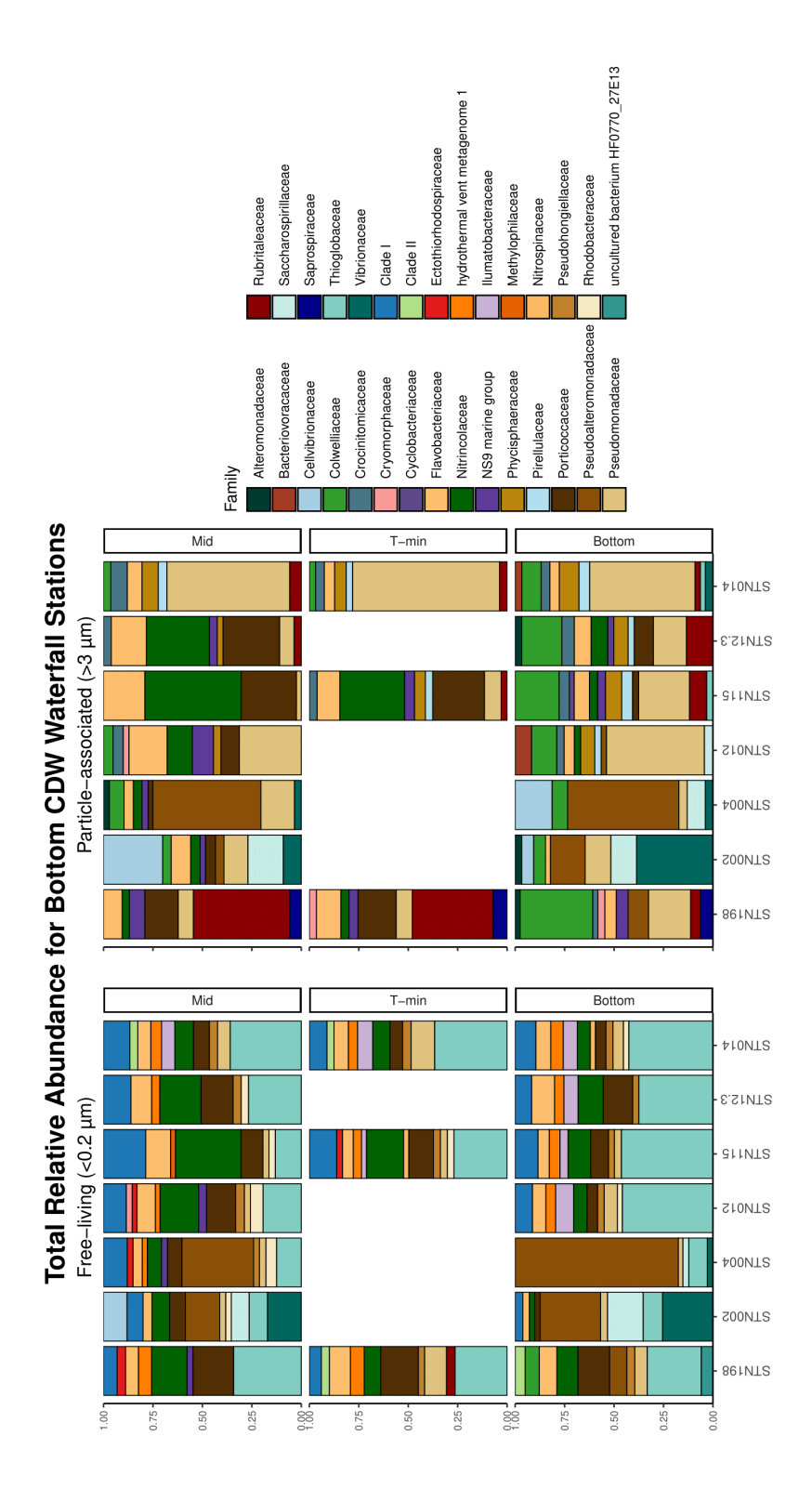


Figure 10. Canonical Correspondence Analysis (CCA) of free-living (A, C) and particle-associated (B, D) bacterial communities based on defined water mass. First row CCAs are surface-200m and bottom row CCAs are 200m-bottom.



**Figure 11.** Relative abundance by water mass and station at the Family level, including Archaea. Similar to previous relative abundance plots (Figure 7; Figure 8) but includes prevalence of *Nitrosopumilaceae*, a known ammonia-oxidizing archaea.



**Figure 12.** Relative abundance of stations coming from off the continental shelf at the family level. Free-living on left and particle-associated on the right.

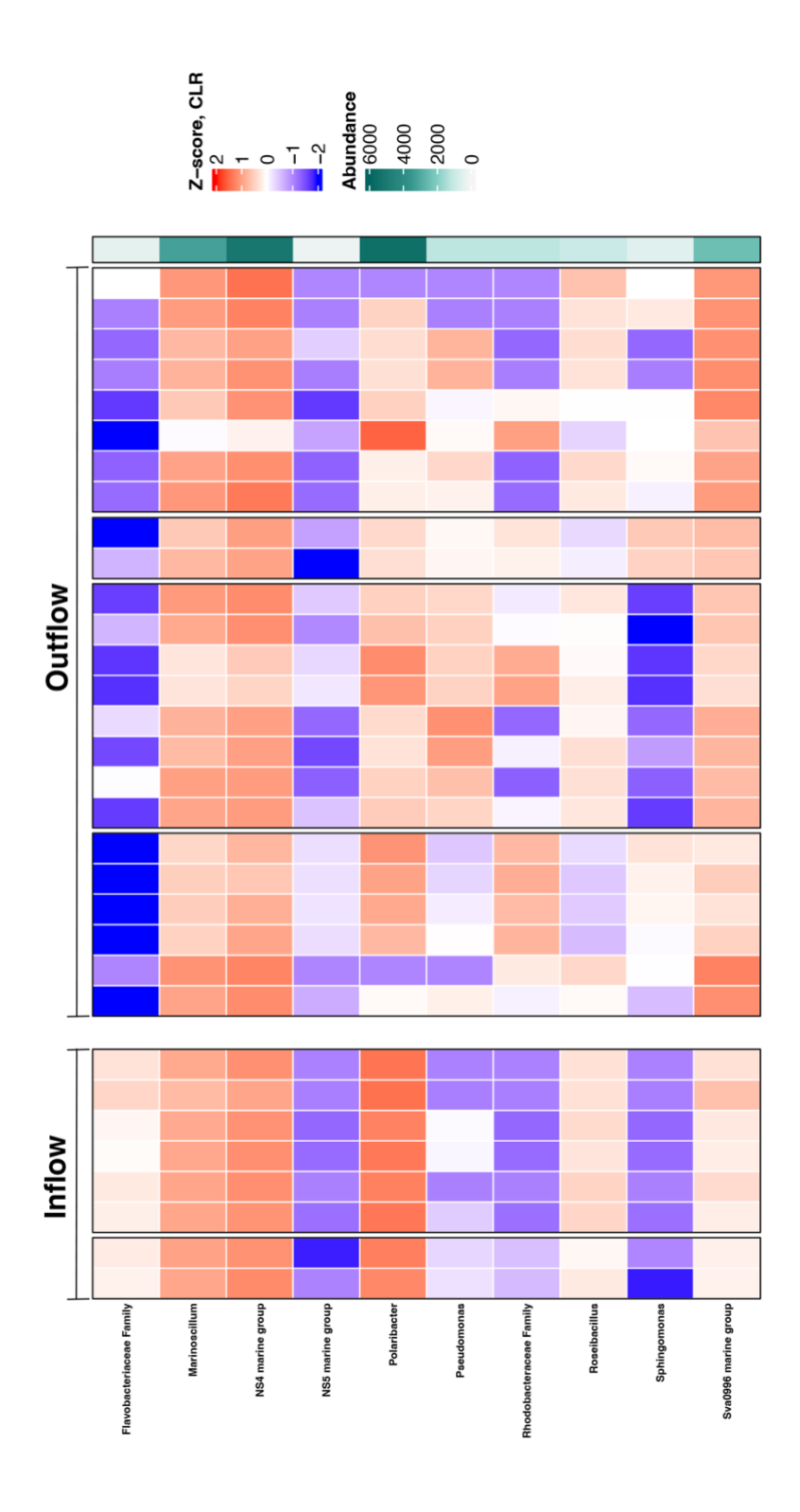


**Figure 13.** Significant **free-living** taxa from ANCOM-BC analysis for inflow vs. outflow samples. Z-score derived from log-transformed data. No significant change in particle-associated taxa from ANCOM-BC analysis.

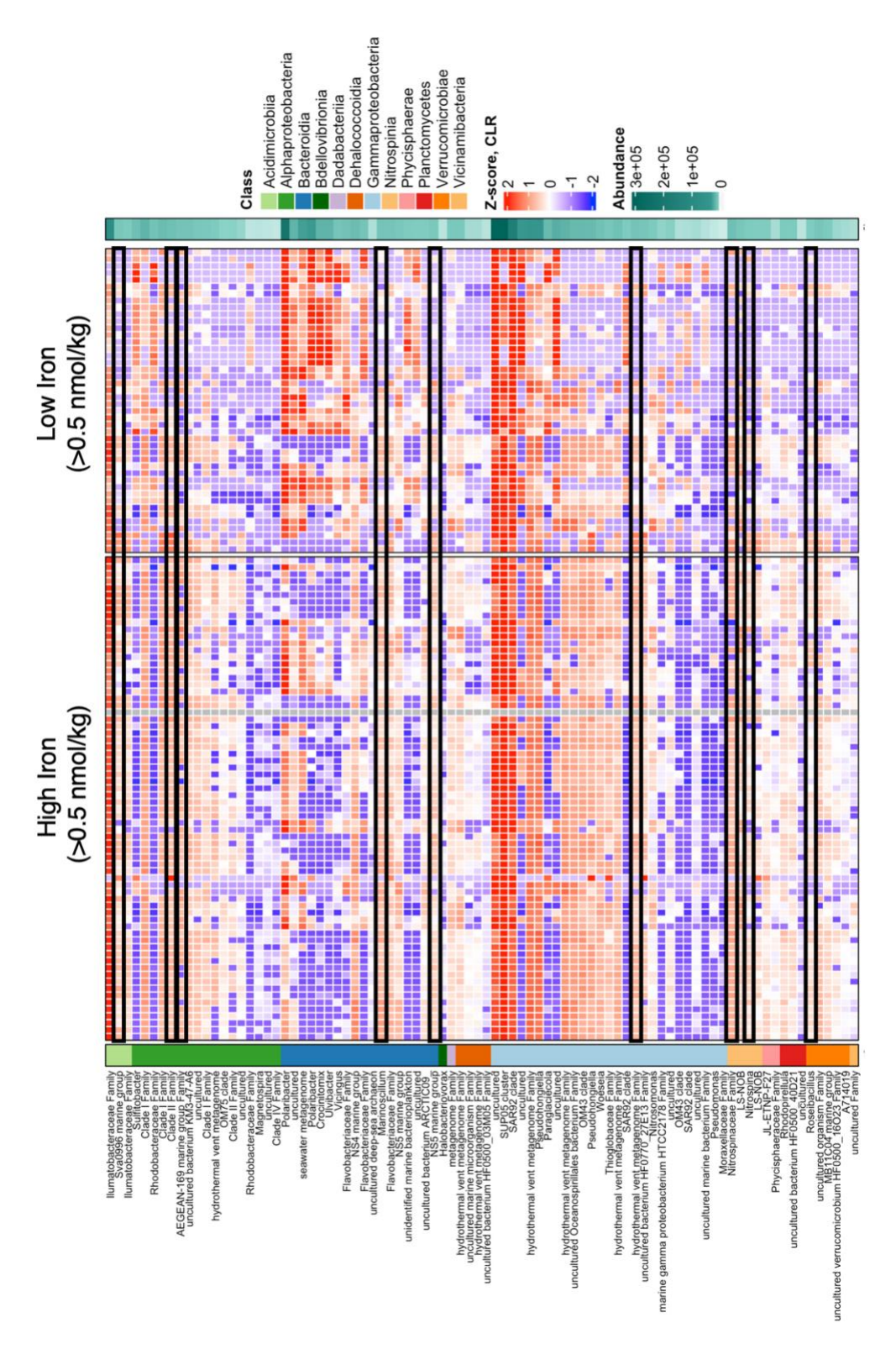


**Figure 14.** Significant **free-living** taxa from ANCOM-BC analysis for high (>0.5 nmol/kg) or low (<0.5 nmol/kg) dFe concentrations. Z-score derived from log-transformed data. Black boxes indicate taxa that are more present in high iron versus low iron.

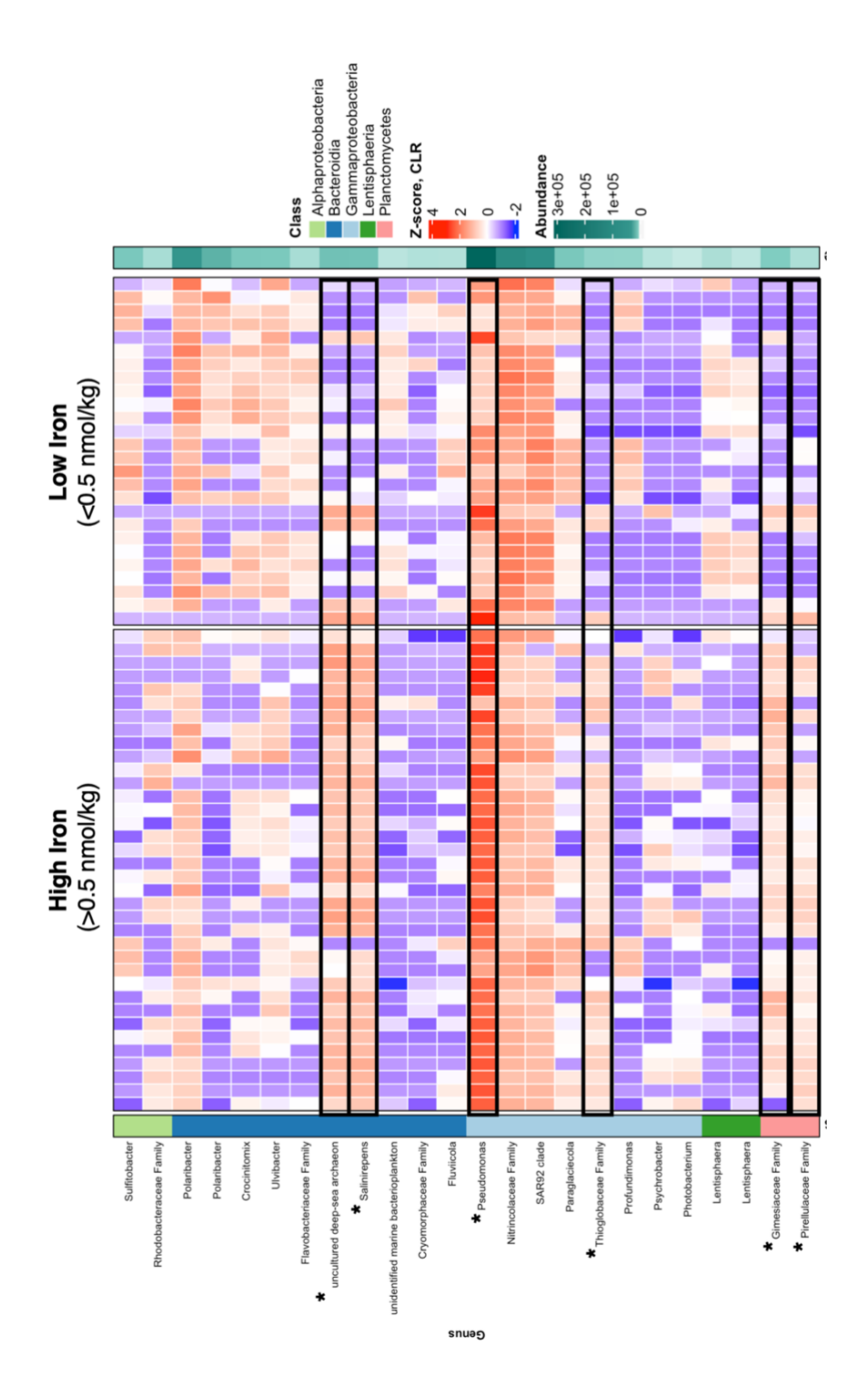


**Figure 15**. Significant **particle-associated** taxa from ANCOM-BC analysis for high (>0.5 nmol/kg) or low (<0.5 nmol/kg) dFe concentrations. Z-score derived from log-transformed data.

## **TABLES**

**Table 1.** Water mass characterization with temperature and salinity ranges.

Water Mass	Temperature Range	Salinity Range
AASW	-1.15 — 0.5	32.75 — 33.87
AASW-WW	-2 — -1.15	33.5 — 33.87
WW	-2 — -1.4	33.88 — 34.5
WW-CDW	-1.4 — 0.1	33.88 — 34.5
CDW	0.1 - 2	33.88 — 35

Table 2. Inflow and outflow stations and depth.

	Station	Latitude	Longitude	Depth
	STN014	-74.23	-112.08	860
	STN014	-74.23	-112.08	700
Inflow	STN014	-74.23	-112.08	580
	STN20	-74.15	-111.9	499
	STN20	-74.15	-111.9	480
	STN22	-74.1753	-113.34488	465
	STN22	-74.1753	-113.34488	325
	STN22	-74.1753	-113.34488	250
	STN22	-74.1753	-113.34488	150
	STN056a	-74.18	-113.34	310
	STN056a	-74.18	-113.34	170
Outflow	STN056a	-74.18	-113.34	150
Outnow	STN056b	-74.18	-113.34	410
	STN056b	-74.18	-113.34	390
	STN056b	-74.18	-113.34	350
	STN056b	-74.18	-113.34	190
	STN068	-74.02906	-113.34464	257
	STN068	-74.02906	-113.34464	190
	STN068	-74.02906	-113.34464	90

**Table 3.** Indicator species analysis of significant taxa in **free-living** outflow community. No significant indicator taxa appeared for particle-associated community.

					erium Family			
Genus	Roseibacillus	Vicingus	uncultured 5	Colwellia	uncultured Oceanospirillales bacterium Family	JL-ETNP-F27	OM43 clade	
Family	Rubritaleaceae	Cryomorphaceae	Cellvibrionaceae	Colwelliaceae	uncultured Oceanospirillales bacterium	Phycisphaeraceae	Methylophilaceae	
Order	Verrucomicrobiales	Flavobacteriales	Cellvibrionales	Alteromonadales	SAR86 clade	Phycisphaerales	Burkholderiales	
Abundance	5.6E-04	2.8E-04	4.2E-06	1.0E-05	4.9E-03	1.1E-03	5.8E-03	
р	0.027	0.015	0.009	0.005	0.009	0.023	0.044	
Flow **	Outflow	Outflow	Outflow	Outflow	Outflow	Outflow	Outflow	
Fract.*	FL	FL	FL	FL	FL	FL	H	
index	2	2	2	2	2	2	2	
ASV#	Seq58	Seq71	Seq78	Seq91	Seq93	Seq94	Seq97	

\* No sig. taxa in outflow for particle-associated. \*\* Sig. taxa in only outflow.

**Table 4.** Indicator species for **free-living** communities based on location, separated into surface-200m (upper 200m) and 200-bottom (below 200m).

								FREE-LIVING	NG.	
Upper 200m	m0									
# ASA	index	OP	West CC	Dotson	Eastern CC	Getz	p.value.bh	Order	Family	Genus
Seq37	8	0	0	0	0	1	0.042	Flavobacteriales	Flavobacteriaceae	Flavobacteriaceae Family
Lower 200m	m0									
ACV #	indox	a	Wort CC	Dotog	Factors CC	100	dd collers a	Copic	raj mez J	anno g
San355	III 1	6	200	1	O	0	0.031	Arctic978-4 marine groun	HF0500 16023	HE0500 16023 Family
Seq235	2	0	0	0	-	0	0.022	Planctomycetales	Gimesiaceae	uncultured 8
Seq447	2	0	0	0	-	0	0.031	Opitutales	Puniceicoccaceae	Pelagicoccus
Seq485	2	0	0	0		0	0.028	nucultured	uncultured marine bacterium	uncultured marine bacterium Family 3
Seq768	2	0	0	0	-	0	0.022	Pedosphaerales	Pedosphaeraceae	Pedosphaeraceae Family
Seq661	3	0	0	0	0	+	0.022	Actinomarinales	Actinomarinaceae	Candidatus Actinomarina
Seq828	6	0	0	0	0	-	0.016	Vicinamibacterales	nucultured	uncultured bacterium AD248-D7-1A
Seq153	4	-	0	0	0	0	0.031	Oceanospirillales	Saccharospirillaceae	Oleispira
Seq171	2	0	-	0	0	0	600.0	Lentisphaerales	Lentisphaeraceae	Lentisphaera
Seq234	0	0	-	0	0	0	0.022	OM182 clade	marine gamma proteobacterium HTCC2178	marine gamma proteobacterium HTCC2178 Family
Seq425	2	0	-	0	0	0	0.016	Cellvibrionales	uncultured marine bacterium	uncultured marine bacterium Family 1
Seq134	9	0	0	-	-	0	0.014	Thiomicrospirales	Thioglobaceae	Thioglobaceae Family
Seq155	9	0	0	-	-	0	0.022	Planctomycetales	nucultured	uncultured bacterium HF0500_40D21
Seq255	9	0	0	-	-	0	0.025	Opitutales	Puniceicoccaceae	MB11C04 marine group
Seq529	9	0	0	-		0	0.022	Defluviicoccales	nucultured	uncultured Parvibaculum sp.
Seq110	7	0	0	-	0	-	0.022	Flavobacteriales	Flavobacteriaceae	NS4 marine group
Seq386	7	0	0	-	0	-	0.031	SAR202 clade	uncultured marine microorganism	uncultured marine microorganism Family 1
Seq161	10	0	0	0		-	0.016	Nitrospinales	Ntrospinaceae	LS-NOB
Seq192	0 9	0	0	0		-	0.022	Sphingomonadales	Sphingomonadaceae	Sphingomonas
Seq444	0 4	,	0 ,	0	- 0	- 0	0.034	Vicinamipacterales	uncurrund	Uncurured Family 1
Sedo	0 4	- 0	- 0	,	-		0.032	CAD11 clode	Porticoccaceae	Olodo II Comily
Seq128	16	0	0	-		-	0.034	Nitrospinales	Nitrospinaceae	Nitrospinaceae Family
Seq132	16	0	0		-	-	0.012	Steroidobacterales	Woeselaceae	Woeseia
Seq144	16	0	0	-		1	0.026	Cytophagales	Cyclobacteriaceae	Marinoscillum
Seq148	16	0	0	•		-	0.031	Rhodospirillales	AEGEAN-169 marine group	AEGEAN-169 marine group Family
Seq156	16	0	0			-	0.025	Defluviicoccales	uncultured	uncultured bacterium KM3-47-A6
Seq185	16	0	0	•	7	-	0.031	Microtrichales	Microtrichaceae	Sva0996 marine group
Seq19	16	0	0	-	-	-	0.044	Microtrichales	llumatobacteraceae	llumatobacteraceae Family
Seq195	16	0	0	-		-	0.031	Rhodospirillales	Magnetospiraceae	uncultured 7
Seq199	16	0	0	-	-	-	0.022	SAR202 clade	hydrothermal vent metagenome	hydrothermal vent metagenome Family 3
Seq260	16	0	0		-	-	0.023	SAR202 clade	uncultured Chloroflex i bacterium HF4000_28F02	uncultured Chloroflexi bacterium HF4000_28F02 Family
Seq34	16	0	0		-	-	0.031	SAR86 clade	hydrothermal vent metagenome	hydrothermal vent metagenome Family 1
Seq38	16	0	0			-	600.0	SAR11 clade	Clade I	Clade I Family
Seq387	16	0	0	-	-	-	0.022	Opitutales	Puniceicoccaceae	A714019
Seq389	16	0	0		-	-	0.034	Thiotrichales	Thiotrichaceae	uncultured 14
Seq563	16	0	0	-	-	-	0.022	SAR202 clade	uncultured bacterium HF0500_03M05	uncultured bacterium HF0500_03M05 Family
Seq616	16	0	0	-	-	-	0.022	Kiloniellales	Kiloniellaceae	uncultured 16
Seq167	56		0				0.039	Flavobacteriales	Flavobacteriaceae	NS5 marine group

**Table 5.** Indicator species for **particle-associated** communities based on location, separated into surface-200m (upper 200m) and 200-bottom (below 200m). No significant taxa for upper 200m.

							ΡĄ	PARTICLE-ASSOCIATED	CIATED	
Upper 200m	00m									
No significant indicator taxa.	ant indica	ator taxa.	_							
Lower 200m	00m									
# ASA	index	OP	West CC	Dotson	Eastern CC	Getz	p.value.bh	Order	Family	Genus
Seq235	2	0	0	0	1	0	0.047	Planctomycetales	Gimesiaceae	uncultured 8
Seq801	2	0	0	0	1	0	0.042	Victivallales	Arctic95B-14	uncultured Verrucomicrobia bacterium
Seq1526	3	0	0	0	0	1	0.027	Methylococcales	Methylomonadaceae	Marine Methylotrophic Group 2
Seq156	3	0	0	0	0	1	0.047	Defluviicoccales	uncultured	uncultured bacterium KM3-47-A6
Seq272	3	0	0	0	0	1	0.033	Phycisphaerales	Phycisphaeraceae	CL500-3
Seq380	3	0	0	0	0	1	0.009	Pirellulales	Pirellulaceae	Pirellulaceae Family
Seq407	3	0	0	0	0	1	600.0	Nannocystales	Nannocystaceae	Nannocystaceae Family
Seq452	3	0	0	0	0	1	0.022	Planctomycetales	Rubinisphaeraceae	uncultured 15
Seq482	3	0	0	0	0	1	0.009	Bradymonadales	uncultured marine bacterium	uncultured marine bacterium Family 2
Seq653	3	0	0	0	0	1	0.027	Oligoflexales	uncultured	uncultured sediment bacterium
Seq171	2	0	1	0	0	0	0.047	Lentisphaerales	Lentisphaeraceae	Lentisphaera
Seq3	2	0	1	0	0	0	0.027	Oceanospirillales	Nitrincolaceae	uncultured 1
Seq420	7	0	0	1	0	1	0.042	Pirellulales	Pirellulaceae	Blastopirellula
Seq95	10	0	0	0	-	-	0.028	Pirellulales	Pirellulaceae	Rhodopirellula
Seq6	15	1	1	0	0	0	0.047	Cellvibrionales	Porticoccaceae	SAR92 clade
Seq1	16	0	0	1	1	-	600.0	Pseudomonadales	Pseudomonadaceae	Pseudomonas
Seq155	16	0	0	-	-	1	0.042	Planctomycetales	uncultured	uncultured bacterium HF0500_40D21

#### REFERENCES

- Alcamán-Arias, María Estrella, Sebastián Fuentes-Alburquenque, Pablo Vergara-Barros,

  Jerónimo Cifuentes-Anticevic, Josefa Verdugo, Martin Polz, Laura Farías, Carlos PedrósAlió, and Beatriz Díez. 2021. "Coastal Bacterial Community Response to Glacier

  Melting in the Western Antarctic Peninsula." *Microorganisms* 9 (1): 1–18.
- Anantharaman, Karthik, John A. Breier, Cody S. Sheik, and Gregory J. Dick. 2013. "Evidence for Hydrogen Oxidation and Metabolic Plasticity in Widespread Deep-Sea Sulfur-Oxidizing Bacteria." *Proceedings of the National Academy of Sciences of the United States of America* 110 (1): 330–35.
- Arrigo, Kevin R., and Gert L. van Dijken. 2003. "Phytoplankton Dynamics within 37 Antarctic Coastal Polynya Systems." *Journal of Geophysical Research* 108 (C8). https://doi.org/10.1029/2002jc001739.
- Bertrand, Erin M., M. Saito, J. Rose, C. Riesselman, M. Lohan, A. Noble, Peter A. Lee, and G.
  R. DiTullio. 2007. "Vitamin B12 and Iron Colimitation of Phytoplankton Growth in the Ross Sea." *Limnology and Oceanography* 52 (May).
  https://doi.org/10.4319/lo.2007.52.3.1079.
- Bowman, John. 2014. "The Family Cryomorphaceae." In . University of Tasmania.
- Bundy, Randelle M., Rene M. Boiteau, Craig McLean, Kendra A. Turk-Kubo, Matt R. McIlvin,
  Mak A. Saito, Benjamin A. S. Van Mooy, and Daniel J. Repeta. 2018. "Distinct
  Siderophores Contribute to Iron Cycling in the Mesopelagic at Station ALOHA."
  Frontiers in Marine Science 5. https://doi.org/10.3389/fmars.2018.00061.

- Casciotti, Karen, Stanford University, Tanya Marshall, Sarah Fawcett, and Angela Knapp. 2024. "Advances in Understanding the Marine Nitrogen Cycle in the GEOTRACES Era." Oceanography 37 (2). https://doi.org/10.5670/oceanog.2024.406.
- Cho, Hyeyoun, Chung Yeon Hwang, Jong-Geol Kim, Sanghoon Kang, Katrin Knittel, Ayeon Choi, Sung-Han Kim, et al. 2020. "A Unique Benthic Microbial Community Underlying the Phaeocystis Antarctica-Dominated Amundsen Sea Polynya, Antarctica: A Proxy for Assessing the Impact of Global Changes." *Frontiers in Marine Science* 6. https://doi.org/10.3389/fmars.2019.00797.
- Debeljak, Pavla, Barbara Bayer, Ying Sun, Gerhard J. Herndl, and Ingrid Obernosterer. 2023. "Seasonal Patterns in Microbial Carbon and Iron Transporter Expression in the Southern Ocean." *Microbiome* 11 (1): 187.
- Delmont, Tom O., A. Murat Eren, Joseph H. Vineis, and Anton F. Post. 2015. "Genome Reconstructions Indicate the Partitioning of Ecological Functions inside a Phytoplankton Bloom in the Amundsen Sea, Antarctica." *Frontiers in Microbiology* 6: 1090.
- Delmont, Tom O., Katherine M. Hammar, Hugh W. Ducklow, Patricia L. Yager, and Anton F. Post. 2014. "Phaeocystis Antarctica Blooms Strongly Influence Bacterial Community Structures in the Amundsen Sea Polynya." *Frontiers in Microbiology* 5 (DEC). https://doi.org/10.3389/fmicb.2014.00646.
- Dinniman, Michael S., Pierre St-Laurent, Kevin R. Arrigo, Eileen E. Hofmann, and Gert L. van Dijken. 2020. "Analysis of Iron Sources in Antarctic Continental Shelf Waters." *Journal of Geophysical Research, C: Oceans* 125 (5). https://doi.org/10.1029/2019JC015736.

- Dinniman, Michael S., 2023. "Sensitivity of the Relationship between Antarctic Ice Shelves and Iron Supply to Projected Changes in the Atmospheric Forcing." *Journal of Geophysical Research, C: Oceans* 128 (2). https://doi.org/10.1029/2022jc019210.
- Ducklow, Hugh W., Stephanie E. Wilson, Anton F. Post, Sharon E. Stammerjohn, Matthew Erickson, Sanghoon Lee, Kate E. Lowry, Robert M. Sherrell, and Patricia L. Yager. 2015. "Particle Flux on the Continental Shelf in the Amundsen Sea Polynya and Western Antarctic Peninsula." *Elementa (Washington, D.C.)* 3 (January): 000046.
- Gerringa, Loes J. A., Anne-Carlijn Alderkamp, Patrick Laan, Charles-Edouard Thuróczy, Hein J. W. De Baar, Matthew M. Mills, Gert L. van Dijken, Hans van Haren, and Kevin R. Arrigo. 2012. "Iron from Melting Glaciers Fuels the Phytoplankton Blooms in Amundsen Sea (Southern Ocean): Iron Biogeochemistry." *Deep-Sea Research. Part II, Topical Studies in Oceanography* 71–76 (September): 16–31.
- Giddy, I. S., S-A Nicholson, B. Y. Queste, S. Thomalla, and S. Swart. 2023. "Sea-ice Impacts Inter-annual Variability of Phytoplankton Bloom Characteristics and Carbon Export in the Weddell Sea." *Geophysical Research Letters* 50 (16). https://doi.org/10.1029/2023g1103695.
- Gwak, Joo-Han, Samuel Imisi Awala, So-Jeong Kim, Sang-Hoon Lee, Eun-Jin Yang, Jisoo Park, Jinyoung Jung, and Sung-Keun Rhee. 2023. "Transcriptomic Insights into Archaeal Nitrification in the Amundsen Sea Polynya, Antarctica." *Journal of Microbiology* 61 (11): 967–80.
- Hogle, Shane L., J. Cameron Thrash, Chris L. Dupont, and Katherine A. Barbeau. 2016. "TraceMetal Acquisition by Marine Heterotrophic Bacterioplankton with Contrasting TrophicStrategies." Applied and Environmental Microbiology 82 (5): 1613–24.

- Jenkins, Adrian, and Stan Jacobs. 2008. "Circulation and Melting beneath George VI Ice Shelf, Antarctica." *JGR Oceans*, April. https://doi.org/10.1029/2007JC004449.
- Kharbush, Jenan J., Hilary G. Close, Benjamin A. S. Van Mooy, Carol Arnosti, Rienk H. Smittenberg, Frédéric A. C. Le Moigne, Gesine Mollenhauer, et al. 2020. "Particulate Organic Carbon Deconstructed: Molecular and Chemical Composition of Particulate Organic Carbon in the Ocean." *Frontiers in Marine Science*. Frontiers Media S.A. https://doi.org/10.3389/fmars.2020.00518.
- Kim, Chang-Sin, Tae-Wan Kim, Kyoung-Ho Cho, Ho Kyung Ha, Sanghoon Lee, Hyun-Cheol Kim, and Jae-Hak Lee. 2016. "Variability of the Antarctic Coastal Current in the Amundsen Sea." *Estuarine, Coastal and Shelf Science* 181 (November): 123–33.
- Kovalevsky, Dmitry V., Igor L. Bashmachnikov, and Genrikh V. Alekseev. 2020. "Formation and Decay of a Deep Convective Chimney." *Ocean Modelling* 148 (April): 101583.
- Liu, Zhengang, Furong Cao, Jiyuan Wan, Xing Chen, Bin Kong, Dong Li, Xiao-Hua Zhang, Yong Jiang, and Xiaochong Shi. 2024. "Stable Microbial Community Diversity across Large-Scale Antarctic Water Masses." *The Science of the Total Environment* 947 (July): 174559.
- Lopez, Chelsea N., and Dennis A. Hansell. 2023. "Anomalous DOC Signatures Reveal Iron Control on Export Dynamics in the Pacific Southern Ocean." *Frontiers in Marine Science* 10. https://doi.org/10.3389/fmars.2023.1070458.
- Ma, Yuhui, Xiangyong Zheng, Shengbing He, and Min Zhao. 2021. "Nitrification,
   Denitrification and Anammox Process Coupled to Iron Redox in Wetlands for Domestic
   Wastewater Treatment." *Journal of Cleaner Production* 300 (10): 126953.

- Martínez-Pérez, Clara, Chris Greening, Sean K. Bay, Rachael J. Lappan, Zihao Zhao, Daniele De Corte, Christina Hulbe, et al. 2022. "Phylogenetically and Functionally Diverse Microorganisms Reside under the Ross Ice Shelf." *Nature Communications* 13 (1): 117.
- Min, Jun-Oh, Sung-Han Kim, Jinyoung Jung, Ui-Jung Jung, Eun Jin Yang, Sanghoon Lee, and Jung-Ho Hyun. 2022. "Glacial Ice Melting Stimulates Heterotrophic Prokaryotes Production on the Getz Ice Shelf in the Amundsen Sea, Antarctica." *Geophysical Research Letters* 49 (19). https://doi.org/10.1029/2021gl097627.
- Morris, Robert M., and Rachel L. Spietz. 2022. "The Physiology and Biogeochemistry of SUP05." *Annual Review of Marine Science* 14 (January): 261–75.
- Parish, Thomas R., and John J. Cassano. 2003. "The Role of Katabatic Winds on the Antarctic Surface Wind Regime." *Monthly Weather Review* 131 (2): 317–33.
- Park, Jiwoon, Bryndan P. Durham, Rebecca S. Key, Ryan D. Groussman, Zinka Bartolek,
  Paulina Pinedo-Gonzalez, Nicholas J. Hawco, et al. 2023. "Siderophore Production and
  Utilization by Marine Bacteria in the North Pacific Ocean." *Limnology and*Oceanography, May. https://doi.org/10.1002/lno.12373.
- Park, Y-H, E. Charriaud, and M. Fieux. 1998. "Thermohaline Structure of the Antarctic Surface Water/Winter Water in the Indian Sector of the Southern Ocean." *Journal of Marine Systems* 17 (1): 5–23.
- Priest, Taylor, Anneke Heins, Jens Harder, Rudolf Amann, and Bernhard M. Fuchs. 2022. "Niche Partitioning of the Ubiquitous and Ecologically Relevant NS5 Marine Group." *The ISME Journal* 16 (6): 1570–82.
- Randall-Goodwin, E., M. P. Meredith, A. Jenkins, P. L. Yager, R. M. Sherrell, E. P. Abrahamsen, R. Guerrero, et al. 2015. "Freshwater Distributions and Water Mass

- Structure in the Amundsen Sea Polynya Region, Antarctica." *Elementa* 3. https://doi.org/10.12952/journal.elementa.000065.
- Richert, Inga, Patricia L. Yager, Julie Dinasquet, Ramiro Logares, Lasse Riemann, Annelie Wendeberg, Stefan Bertilsson, and Douglas G. Scofield. 2019. "Summer Comes to the Southern Ocean: How Phytoplankton Shape Bacterioplankton Communities Far into the Deep Dark Sea." *Ecosphere* 10 (3). https://doi.org/10.1002/ecs2.2641.
- Scambos, T. A., R. E. Bell, R. B. Alley, S. Anandakrishnan, D. H. Bromwich, K. Brunt, K. Christianson, et al. 2017. "How Much, How Fast?: A Science Review and Outlook for Research on the Instability of Antarctica's Thwaites Glacier in the 21st Century." *Global and Planetary Change*. Elsevier B.V. https://doi.org/10.1016/j.gloplacha.2017.04.008.
- Schine, Casey M. S., Anne-Carlijn Alderkamp, Gert van Dijken, Loes J. A. Gerringa, Sara Sergi,
  Patrick Laan, Hans van Haren, Willem H. van de Poll, and Kevin R. Arrigo. 2021.

  "Massive Southern Ocean Phytoplankton Bloom Fed by Iron of Possible Hydrothermal
  Origin." *Nature Communications* 12 (1): 1211.
- Silvano, Alessandro, Stephen Rich Rintoul, Beatriz Peña-Molino, William Richard Hobbs, Esmee van Wijk, Shigeru Aoki, Takeshi Tamura, and Guy Darvall Williams. 2018. "Freshening by Glacial Meltwater Enhances Melting of Ice Shelves and Reduces Formation of Antarctic Bottom Water." *Science Advances* 4 (4): eaap9467.
- St-Laurent, P., P. L. Yager, R. M. Sherrell, S. E. Stammerjohn, and M. S. Dinniman. 2017. "Pathways and Supply of Dissolved Iron in the Amundsen Sea (Antarctica)." *Journal of Geophysical Research, C: Oceans* 122 (9): 7135–62.
- Teeling, Hanno, Bernhard M. Fuchs, Dörte Becher, Christine Klockow, Antje Gardebrecht,
  Christin M. Bennke, Mariette Kassabgy, et al. 2012. "Substrate-Controlled Succession of

- Marine Bacterioplankton Populations Induced by a Phytoplankton Bloom." *Science* 336 (6081): 608–11.
- Thiele, Stefan, Julia E. Storesund, Mar Fernández-Méndez, Philipp Assmy, and Lise Øvreås.

  2022. "A Winter-to-Summer Transition of Bacterial and Archaeal Communities in Arctic Sea Ice." *Microorganisms* 10 (8). https://doi.org/10.3390/microorganisms10081618.
- Thiele, Stefan, Anna Vader, Stuart Thomson, Karoline Saubrekka, Elzbieta Petelenz, Hilde Rief Armo, Oliver Müller, Lasse Olsen, Gunnar Bratbak, and Lise Øvreås. 2023. "The Summer Bacterial and Archaeal Community Composition of the Northern Barents Sea." *Progress in Oceanography* 215 (July): 103054.
- Tremblay, J-E, and W. O. Smith. 2007. "Chapter 8 Primary Production and Nutrient Dynamics in Polynyas." In *Elsevier Oceanography Series*, edited by W. O. Smith and D. G. Barber, 74:239–69. Elsevier.
- Wang, Bo, Lingfang Fan, Minfang Zheng, Yusheng Qiu, and Min Chen. 2022. "Carbon and Iron Uptake by Phytoplankton in the Amundsen Sea, Antarctica." *Biology* 11 (12). https://doi.org/10.3390/biology11121760.
- Yager, Patricia L., Robert M. Sherrell, Sharon E. Stammerjohn, Anne Carlijn Alderkamp, Oscar Schofield, E. Povl Abrahamsen, Kevin R. Arrigo, et al. 2012. "ASPIRE: The Amundsen Sea Polynya International Research Expedition." *Oceanography* 25 (3): 40–53.
- Yang, H. W., T-W Kim, Pierre Dutrieux, A. K. Wåhlin, Adrian Jenkins, H. K. Ha, C. S. Kim, et al. 2022. "Seasonal Variability of Ocean Circulation near the Dotson Ice Shelf, Antarctica." *Nature Communications* 13 (1): 1138.

Žure, Marina, Antonio Fernandez-Guerra, Colin B. Munn, and Jens Harder. 2017. "Geographic Distribution at Subspecies Resolution Level: Closely Related Rhodopirellula Species in European Coastal Sediments." *The ISME Journal* 11 (2): 478–89.

## APPENDIX – SUPPLEMENTARY TABLES

Table S1. Taxonomy table for unique taxonomic ranks going to species.

Phylum	Order	Family	Genus	Species
Proteobacteria	Oceanospirillales	Alcanivoracaceae	Alcanivorax	Alcanivorax Genus
Proteobacteria	Alteromonadales	Alteromonadaceae	Paraglaciecola	Paraglaciecola Genus
Bdellovibrionota	Bacteriovoracales	Bacteriovoracaceae	uncultured	hydrothermal vent metagenome
Proteobacteria	Cellvibrionales	Cellvibrionaceae	uncultured	gamma proteobacterium NEP2
Proteobacteria	SAR11 clade	Clade I	Clade I Family	Clade I Family
Proteobacteria	SAR11 clade	Clade I	Clade Ia	Clade la Genus
Proteobacteria	SAR11 clade	Clade II	Clade II Family	Clade II Family
Proteobacteria	Alteromonadales	Colwelliaceae	Colwellia	Colwellia Genus
Proteobacteria	Alteromonadales	Colwelliaceae	Colwelliaceae Family	Colwelliaceae Family
Bacteroidota	Flavobacteriales	Crocinitomicaceae	Crocinitomicaceae Family	Crocini tomicaceae Family
Bacteroidota	Flavobacteriales	Crocinitomicaceae	Fluviicola	marin e metagenome
Bacteroidota	Flavobacteriales	Crocinitomicaceae	Salinirepens	uncultured bacterium
Bacteroidota	Flavobacteriales	Crocinitomicaceae	Fluviicola	uncultured Bacteroidetes/Chlorobi group bacterium
Bacteroidota	Flavobacteriales	Crocinitomicaceae	Crocinitomix	uncultured marine bacterium
Bacteroidota	Flavobacteriales	Crocinitomicaceae	Salinirepens	uncultured marine bacterium
Bacteroidota	Flavobacteriales	Cryomorphaceae	uncultured	uncultured Genus
Bacteroidota	Flavobacteriales	Cryomorphaceae	Vicingus	Vicingus Genus
Proteobacteria	Ectothiorhodospirales	Ectothiorhodospiraceae	uncultured	uncultured proteobacterium
Bacteroidota	Flavobacteriales	Flavobacteriaceae	uncultured	Aquimarina versatilis
Bacteroidota	Flavobacteriales	Flavobacteriaceae	uncultured	Flav obacteriaceae bacterium 14III/A01/012
Bacteroidota	Flavobacteriales	Flavobacteriaceae	Flav obacteriaceae Family	Flavobacteriaceae Family
Bacteroidota	Flavobacteriales	Flavobacteriaceae	Polaribacter	Polaribacter Genus
Bacteroidota	Flavobacteriales	Flavobacteriaceae	Ulvibacter	uncultured bacterium ARCTIC16_F_12
Bacteroidota	Flavobacteriales	Flavobacteriaceae	uncultured	uncultured Genus
Planctomycetota	Planctomycetales	Gimesiaceae	uncultured	uncultured Planctomyces clone 7F15
Proteobacteria	Oceanospirillales	Halomonadaceae	Halomonas	Halo monas Genus
Actinobacteriota	Microtrichales	Ilumatobacteraceae	Ilumatobacteraceae Family	Ilumatob acteraceae Family
Bacteroidota	Sphingobacteriales	Lentimicrobiaceae	uncultured deep-sea archaeon	uncultured deep-s ea archaeon Genus
Proteobacteria	Alteromonadales	Marinobacteraceae	Marinobacter	Marinobacter Genus
Proteobacteria	Nitrosococcales	Methylophagaceae	Methylophagaceae Family	Methylophagaceae Family
Proteobacteria	Pseudomonadales	Moraxellaceae	Psychrobacter	Psychrobacter Genus

Phylum	Order	Family	Genus	Species
Proteobacteria	Alteromonadales	Moritellaceae	Moritella	Moritella Genus
Bacteroidota	Flavobacteriales	NS9 marine group	NS9 marine group Family	NS9 marine group Family
Bacteroidota	Flavobacteriales	NS9 marine group	seawater metagenome	seawater metagenome Genus
Bacteroidota	Flavobacteriales	NS9 marine group	uncultured Flavobacterium sp.	uncultured Flavobacterium sp. Genus
Proteobacteria	Oceanospirillales	Nitrincolaceae	uncultured	mari ne metagenome
Proteobacteria	Oceanospirillales	Nitrincolaceae	Profundimonas	Profundimonas Genus
Proteobacteria	Oceanospirillales	Nitrincolaceae	uncultured	seawater metagenome
Crenarchaeota	Nitrosopumilales	Nitrosopumilaceae	Candidatus Nitrosopumilus	Candidatus Nitrosopumilus Genus
Crenarchaeota	Nitrosopumilales	Nitrosopumilaceae	Nitrosopumilaceae Family	Nitro so pumilaceae Family
Crenarchaeota	Nitrosopumilales	Nitrosopumilaceae	Candidatus Nitrosopumilus	Thaumarchaeota archaeon SCGC AAA282-K18
Crenarchaeota	Nitrosopumilales	Nitrosopumilaceae	uncultured crenarchaeote ODPB-A3	uncultured crenarchaeote ODPB-A3 Genus
Crenarchaeota	Nitrosopumilales	Nitrosopumilaceae	uncultured eury archaeote	uncultured eury archaeote Genus
Crenarchaeota	Nitrosopumilales	Nitrosopumilaceae	uncultured marine crenarchaeote SAT1000-49-D2	uncultured marine crenarchaeote SATI 000-49- D2 Genus
Crenarchaeota	Nitrosopumilales	Nitrosopumilaceae	uncultured marine thaumarchaeote KM3_69_H10	uncultured marine thaumarchaeote KM3_69_H10 Genus
Planctomycetota	Phycisphaerales	Phycisphaeraceae	JL-ETNP-F27	uncultured deep-sea bacterium
Planctomycetota	Pirellulales	Pirellulaceae	Rhodopirellula	hydrothermal vent metagenome
Proteobacteria	Cellvibrionales	Porticoccaceae	SAR92 clade	SAR92 clade Genus
Proteobacteria	Alteromonadales	Pseudoalteromonadaceae	Pseudoalteromonadaceae Family	Pseudo altero monadaceae Family
Proteobacteria	Alteromonadales	Pseudoalteromonadaceae	Pseudoalteromonas	Pseudoalteromonas Genus
Proteobacteria	Oceanospirillales	Pseudohongiellaceae	Pseudohongiella	marine gamma proteobacterium HTCC2188
Proteobacteria	Oceanospirillales	Pseudohongiellaceae	Pseudohongiella	Pseudohongiella Genus
Proteobacteria	Oceanospirillales	Pseudohongiellaceae	Pseudohongiella	seawater metagenome
Proteobacteria	Pseudomonadales	Pseudomonadaceae	Pseudomonas	Pseudomonas Genus
Proteobacteria	Rhizobiales	Rhizobiaceae	Hoeflea	Hoeflea Genus
Proteobacteria	Rhodobacterales	Rhodobacteraceae	Rhodobacteraceae Family	Rhodobacteraceae Family
Proteobacteria	Rhodobacterales	Rhodobacteraceae	Sulfitobacter	Sulfitobacter Genus
Verrucomicrobiota	Verrucomicrobiales	Rubritaleaceae	Roseibacillus	Roseibacillus Genus
Verrucomicrobiota	Verrucomicrobiales	Rubritaleaceae	Luteolibacter	uncultured organism
Verrucomicrobiota	Verrucomicrobiales	Rubritaleaceae	Roseibacillus	uncultured Roseibacillus sp.
Proteobacteria	Oceanospirillales	Saccharospirillaceae	Oleispira	Oleispira Genus

Phylum	Order	Family	Genus	Species
Proteobacteria	Oceanospirillales	Saccharospirillaceae	Saccharospirillaceae Family	Saccharospirillaceae Family
Proteobacteria	Oceanospirillales	Saccharospirillaceae	uncultured	uncultured Oceano spirillales bacterium
Bacteroidota	Chitinophagales	Saprospiraceae	Lewinella	Lewinella Genus
Bacteroidota	Chitinophagales	Saprospiraceae	Aureispira	Saprospira sp. CNJ640
Bacteroidota	Chitinophagales	Saprospiraceae	Saprospiraceae Family	Saprospiraceae Family
Bacteroidota	Chitinophagales	Saprospiraceae	Aureispira	uncultured marine bacterium
Bacteroidota	Chitinophagales	Saprospiraceae	Lewinella	uncultured marine bacterium
Proteobacteria	Sphingomonadales	Sphingomonadaceae	Sphingomonadaceae Family	Sphingomonadaceae Family
Proteobacteria	Thiomicrospirales	Thioglobaceae	SUP05 cluster	SUP05 cluster Genus
Proteobacteria	Thiomicrospirales	Thioglobaceae	Thioglobaceae Family	Thioglobaceae Family
Proteobacteria	Vibrionales	Vibrionaceae	Vibrion aceae Family	Vi bri onaceae Fami ly
Thermoplasmatota	Marine Group II	hydrothermal vent metagenome	hydrothermal vent metagenome Family	hy drothermal vent metagenome Family
Proteobacteria	SAR86 clade	hydrothermal vent metagenome	hydrothermal vent metagenome Family	hy drothermal vent metagenome Family
Proteobacteria	HOC36	uncultured bacterium HF0770_27E13	uncultured bacterium HF0770_27E13 Family	uncultured bacterium HF0770_27E13 Family
Patescibacteria	Candidatus Kaiserbacteria	uncultured prokaryote	uncultured prokary ote Family	uncultured prokaryote Family

Table S2. Metadata table for size-fractionation and environmental data for each sample.

	Size		Latitude	Longitude	Practical	Potential	Depth	NO3-	PO4	NO2	NH4	02	DOC	Iron
эашыс	Fract.	Station	(deg S)	(deg W)	Salinity	Temp. (°C)	(m)	(µmol/L)	$(\mu mol/L)$	$(\mu mol/L)$	(µmol/L)	(mL/L)	(μM)	(nmol/kg)
STN002.517.pre.poly.3.LG	PA	2	72.20	117.69	34.7	6.0	517	33.6	2.26	0.02	0.27	4.5	43	0.42
STN002.517.fil.dura.r1	ЪГ	2	72.20	117.69	34.7	6.0	517	33.6	2.26	0.02	0.27	4.5	43	0.42
STN002.517.fil.dura.r2	FL	2	72.20	117.69	34.7	6.0	517	33.6	2.26	0.02	0.27	4.5	43	0.42
STN002.200.pre.poly.3.LG	PA	2	72.20	117.69	34.1	-1.7	300	31.5	2.16	0.04	80.0	6.5	49	-
STN002.200.fil.dura.rl	FL	2	72.20	117.69	34.1	-1.7	300	31.5	2.16	0.04	80.0	6.5	49	-
STN002.200.fil.dura.r2	FL	2	72.20	117.69	34.1	-1.7	300	31.5	2.16	0.04	80.0	6.5	49	-
STN002.20.pre.poly.3.LG	PA	2	72.20	117.69	33.5	9.0-	20	9.2	28.0	80.0	0.41	9.4	65	
STN002.20.fil.dura.r1	H	2	72.20	117.69	33.5	9.0-	20	9.2	18.0	80.0	0.41	9.4	65	
STN002.20.fil.dura.r2	FL	2	72.20	117.69	33.5	9.0-	20	9.2	18.0	80.0	0.41	9.4	65	-
STN004.555.pre.poly.3.LG	PA	4	73.14	113.95	34.6	9.0	555	33.9	2.27	0.03	0.03	4.6	42	0.48
STN004.555.fil.dura.rl	FL	4	73.14	113.95	34.6	9.0	555	33.9	2.27	0.03	0.03	4.6	42	0.48
STN004.555.fil.dura.r2	ЪГ	4	73.14	113.95	34.6	9.0	555	33.9	2.27	0.03	0.03	4.6	42	0.48
STN004.300.pre.poly.3.LG	PA	4	73.14	113.95	34.1	-1.8	300	31.9	2.15	0.03	0.12	9.9	42	-
STN004.300.fil.dura.rl	FL	4	73.14	113.95	34.1	-1.8	300	31.9	2.15	0.03	0.12	9.9	42	:
STN004.300.fil.dura.r2	FL	4	73.14	113.95	34.1	-1.8	300	31.9	2.15	0.03	0.12	9.9	42	-
STN004.30.pre.poly.3.LG	PA	4	73.14	113.95	33.9	-0.4	30	17.0	1.42	0.07	0.65	9.8	53	1
STN004.30.fil.dura.rl	FL	4	73.14	113.95	33.9	-0.4	30	17.0	1.42	0.07	0.65	9.8	53	1
STN004.30.fil.dura.r2	FL	4	73.14	113.95	33.9	-0.4	30	17.0	1.42	0.07	0.65	9.8	53	1
STN012.730.pre.poly.3.LG	PA	12	73.80	112.67	34.6	9.0	730	34.1	2.3	0.02	0.13	4.6	40	1.17
STN012.730.fil.dura.r1	FL	12	73.80	112.67	34.6	9.0	730	34.1	2.3	0.02	0.13	4.6	40	1.17
STN012.730.fi1.dura.r2	FL	12	73.80	112.67	34.6	9.0	730	34.1	2.3	0.02	0.13	4.6	40	1.17
STN012.300.pre.poly.3.LG	PA	12	73.80	112.67	34.1	-1.8	300	31.9	2.17	0.07	0.11	6.7	42	0.37
STN012.300.fi1.dura.r1	FL	12	73.80	112.67	34.1	-1.8	300	31.9	2.17	70.0	0.11	2.9	42	0.37
STN012.300.fi1.dura.r2	FL	12	73.80	112.67	34.1	-1.8	300	31.9	2.17	0.07	0.11	6.7	42	0.37
STN012.30.pre.poly.3.LG	PA	12	73.80	112.67	33.8	9.0-	30	18.3	1.5	70.0	0.43	9.8	48	0.11
STN012.30.fil.dura.rl	FL	12	73.80	112.67	33.8	9.0-	30	18.3	1.5	0.07	0.43	8.8	48	0.11
STN012.30.fil.dura.r2	FL	12	73.80	112.67	33.8	9.0-	30	18.3	1.5	0.07	0.43	8.8	48	0.11
STN014.860.pre.poly.3.LG	PA	14	74.23	112.08	34.5	0.4	098	34.9	2.39	0.06	0.15	4.6	44	0.83
STN014.860.fi1.dura.r1	FL	14	74.23	112.08	34.5	0.4	860	34.9	2.39	0.06	0.15	4.6	44	0.83
STN014.860.fi1.dura.r2	FL	14	74.23	112.08	34.5	0.4	098	34.9	2.39	0.06	0.15	4.6	44	0.83
STN014.700.pre.poly.3.LG	PA	14	74.23	112.08	34.5	0.4	700	34.1	2.37	90.0	0.14	4.6	50	0.91

Sample STN014.700.fil.dura.rl		_	Latitude	Longitude	Practical	Potential	Depth	NO3-	PO4	NO2	NH4	02	D0C	Iron
STN014.700.fil.dura.r1	Fract.	Station	(deg S)	(deg W)	Salinity	Temp. (°C)	(m)	(µmol/L)	(mmol/L)	(µmol/L)	(mmol/L)	(mL/L)	(μM)	(nmol/kg)
	FL	14	74.23	112.08	34.5	0.4	700	34.1	2.37	90.0	0.14	4.6	50	0.91
STN014.700.fil.dura.r2	FL	14	74.23	112.08	34.5	0.4	700	34.1	2.37	90.0	0.14	9.4	50	0.91
STN014.580.pre.poly.3.LG	PA	14	74.23	112.08	34.4	0.1	580	33.7	2.29	0	60.0	4.7	48	0.53
STN014.580.fil.dura.rl	FL	14	74.23	112.08	34.4	0.1	580	33.7	2.29	0	60:0	4.7	48	0.53
STN014.580.fil.dura.r2	FL	14	74.23	112.08	34.4	0.1	580	33.7	2.29	0	0.09	4.7	48	0.53
STN014.460.pre.poly.3.LG	PA	14	74.23	112.08	34.4	0.0	460	33.7	2.27	0	0.03	4.7	49	0.57
STN014.460.fil.dura.rl	FL	14	74.23	112.08	34.4	0.0	460	33.7	2.27	0	0.03	4.7	49	0.57
STN014.460.fil.dura.r2	FL	14	74.23	112.08	34.4	0.0	460	33.7	2.27	0	0.03	4.7	49	0.57
STN014.300.pre.poly.3.LG	PA	14	74.23	112.08	34.1	-1.4	300	31.8	2.18	0.01	0.11	6.2	44	0.68
STN014.300.fil.dura.rl	FL	14	74.23	112.08	34.1	-1.4	300	31.8	2.18	0.01	0.11	6.2	44	89.0
STN014.300.fil.dura.r2	FL	14	74.23	112.08	34.1	-1.4	300	31.8	2.18	0.01	0.11	6.2	44	89.0
STN014.40.pre.poly.3.LG	PA	14	74.23	112.08	33.8	-1.1	40	26.6	1.87	90.0	0.16	2.7	46	0.14
STN014.40.fil.dura.r1	FL	14	74.23	112.08	33.8	-1.1	40	26.6	1.87	90.0	0.16	5.7	46	0.14
STN014.40.fil.dura.r2	FL	14	74.23	112.08	33.8	-1.1	40	26.6	1.87	90.0	0.16	7.5	46	0.14
STN20.499.pre.poly.3.LG	PA	20	74.15	111.9	34.4	0.1	499	33.7	2.32	0.01	80.0	4.8	40	0.51
STN20.499.fil.dura.r1	FL	20	74.15	111.9	34.4	0.1	499	33.7	2.32	0.01	0.08	8.4	40	0.51
STN20.499.fil.dura.r2	FL	20	74.15	111.9	34.4	0.1	499	33.7	2.32	0.01	0.08	4.8	40	0.51
STN20.175.pre.poly.3.LG	PA	20	74.15	111.9	34.0	-1.5	175	30.9	2.12	0.06	0.23	6.4	39	0.41
STN20.175.fil.dura.r1	FL	20	74.15	111.9	34.0	-1.5	175	30.9	2.12	90.0	0.23	6.4	39	0.41
STN20.175.fil.dura.r2	FL	20	74.15	111.9	34.0	-1.5	175	30.9	2.12	90.0	0.23	6.4	39	0.41
STN20.25.pre.poly.3.LG	PA	20	74.15	111.9	33.8	-1.2	25	26.6	1.86	0.04	0.18	9.7	78	0.16
STN20.25.fil.dura.r1	FL	20	74.15	111.9	33.8	-1.2	25	26.6	1.86	0.04	0.18	7.6	78	0.16
STN20.25.fil.dura.r2	FL	20	74.15	111.9	33.8	-1.2	25	26.6	1.86	0.04	0.18	7.6	78	0.16
STN198.20.fil.poly.S	FL	198	72.00	119.4	33.2	-1.1	20	13.6	1.19	60.0	2.07	8.3	58	0.16
STN22.610.pre.poly.3.LG	PA	22	74.18	113.34	34.4	0.1	610	33.4	2.3	0.01	0.05	4.7	44	0.52
STN22.610.fil.dura.r1	FL	22	74.18	113.34	34.4	0.1	610	33.4	2.3	0.01	0.05	4.7	44	0.52
STN22.610.fil.dura.r2	FL	22	74.18	113.34	34.4	0.1	610	33.4	2.3	0.01	0.05	4.7	44	0.52
STN22.465.pre.poly.3.LG	PA	22	74.18	113.34	34.3	-0.1	465	33.4	2.3	0	0.08	4.8	41	0.64
STN22.465.fil.dura.r1	FL	22	74.18	113.34	34.3	-0.1	465	33.4	2.3	0	0.08	4.8	41	0.64
STN22.465.fil.dura.r2	FL	22	74.18	113.34	34.3	-0.1	465	33.4	2.3	0	0.08	4.8	41	0.64
STN22.325.pre.poly.3.LG	PA	22	74.18	113.34	34.2	-0.5	325	33.3	2.29	0.01	0.12	4.9	42	0.57

	Size		Latitude	Longitude	Practical	Potential	Depth	NO3-	PO4	NO2	NH4	02	DOC	Iron
Sample	Fract.	Station	(deg S)	(deg W)	Salinity	Temp. (°C)	(m)	(µmol/L)	(µmol/L)	(mmol/L)	(µmol/L)	(mL/L)	(µM)	(nmol/kg)
STN22.325.fil.dura.rl	H	22	74.18	113.34	34.2	-0.5	325	33.3	2.29	0.01	0.12	4.9	42	0.57
STN22.325.fil.dura.r2	FL	22	74.18	113.34	34.2	-0.5	325	33.3	2.29	0.01	0.12	4.9	42	0.57
STN22.250.pre.poly.3.LG	PA	22	74.18	113.34	34.1	7.0-	250	33.2	2.28	0	90.0	5.0	44	0.57
STN22.250.fil.dura.rl	FL	22	74.18	113.34	34.1	7.0-	250	33.2	2.28	0	90.0	5.0	44	0.57
STN22.250.fil.dura.r2	FL	22	74.18	113.34	34.1	7.0-	250	33.2	2.28	0	90.0	5.0	44	0.57
STN22.150.pre.poly.3.LG	PA	22	74.18	113.34	34.0	6.0-	150	33.1	2.29	0.01	80.0	5.1	39	0.62
STN22.150.fil.dura.rl	FL	22	74.18	113.34	34.0	-1.0	150	33.1	2.29	0.01	0.08	5.1	39	0.62
STN22.150.fil.dura.r2	FL	22	74.18	113.34	34.0	-1.0	150	33.1	2.29	0.01	0.08	5.1	39	0.62
STN22.2.pre.poly.3.LG	PA	22	74.18	113.34	33.9	-1.3	2	32.4	2.25	0.02	80.0	5.5	38	0.73
STN22.2.fil.dura.r1	FL	22	74.18	113.34	33.9	-1.3	2	32.4	2.25	0.02	80.0	5.5	38	0.73
STN22.2.fil.dura.r2	FL	22	74.18	113.34	33.9	-1.3	2	32.4	2.25	0.02	80.0	5.5	38	0.73
STN056a.310.pre.poly.3.LG	PA	56a	74.18	113.34	34.2	9.0-	310	33.3	2.24	0.01	0.18	5.0	42	0.64
STN056a.310.fil.dura.rl	FL	56a	74.18	113.34	34.2	9.0-	310	33.3	2.24	0.01	0.18	5.0	42	0.64
STN056a.310.fil.dura.r2	FL	56a	74.18	113.34	34.2	9.0-	310	33.3	2.24	0.01	0.18	5.0	42	0.64
STN056a.170.pre.poly.3.LG	PA	56a	74.18	113.34	34.0	-1.3	170	32.6	2.2	0.02	60.0	5.7	42	0.59
STN056a.170.fil.dura.rl	FL	56a	74.18	113.34	34.0	-1.2	170	32.6	2.2	0.02	60.0	5.5	42	0.59
STN056a.170.fil.dura.r2	FL	56a	74.18	113.34	34.0	-1.2	170	32.6	2.2	0.02	60.0	5.5	42	0.59
STN056a.150.pre.poly.3.LG	PA	56a	74.18	113.34	33.9	-1.3	150	32.6	2.18	0.02	0.15	5.4	45	0.75
STN056a.150.fil.dura.rl	FL	56a	74.18	113.34	33.9	-1.3	150	32.6	2.18	0.02	0.15	5.4	45	0.75
STN056a.150.fil.dura.r2	FL	56a	74.18	113.34	33.9	-1.3	150	32.6	2.18	0.02	0.15	5.4	45	0.75
STN056a.100.pre.poly.3.LG	PA	56a	74.18	113.34	33.9	-1.4	100	32.6	2.19	0.02	0.15	5.4	50	
STN056a.100.fil.dura.r1	FL	56a	74.18	113.34	33.9	-1.4	100	32.6	2.19	0.02	0.15	5.4	50	
STN056a.100.fil.dura.r2	FL	56a	74.18	113.34	33.9	-1.4	100	32.6	2.19	0.02	0.15	5.4	50	-
STN056b.410.pre.poly.3.LG	PA	56b	74.18	113.34	34.3	-0.3	410	-	-	-	-	4.9		0.64
STN056b.410.fil.dura.r1	FL	56b	74.18	113.34	34.3	-0.3	410	:		1	1	4.9		0.64
STN056b.410.fil.dura.r2	FL	56b	74.18	113.34	34.3	-0.3	410	:	-	1	1	4.9		0.64
STN056b.390.pre.poly.3.LG	PA	56b	74.18	113.34	34.3	-0.4	390	:		1	1	5.0		0.58
STN056b.390.fil.dura.r1	FL	56b	74.18	113.34	34.3	-0.4	390	:		1	1	5.0		0.58
STN056b.390.fil.dura.r2	FL	26b	74.18	113.34	34.3	-0.4	390	1	;	1	;	5.0	1	0.58
STN056b.350.pre.poly.3.LG	PA	26b	74.18	113.34	34.2	-0.5	350	1	1	1	1	5.0	;	0.63
STN056b.350.fil.dura.rl	딢	56b	74.18	113.34	34.2	-0.5	350	1	1	1	;	5.0	1	0.63

,	Size		Latitude	Longitude	Practical	Potential	Depth	NO3-	P04	NO2	NH4	02	DOC	Iron
Sample	Fract.	Station	(S gab)	(deg W)	Salinity	Temp. (°C)	(m)	(µmol/L)	(mmol/L)	(µmol/L)	$(\mu mol/L)$	(mL/L)	(μM)	(nmol/kg)
STN056b.350.fil.dura.r2	H	995	74.18	113.34	34.2	-0.5	350		:			0.3		0.63
STN056b.190.pre.poly.3.LG	PA	56b	74.18	113.34	34.0	-1.2	190		-	-		5.4		0.54
STN056b.190.fil.dura.rl	문	56b	74.18	113.34	34.0	-1.2	190	:	1		-	5.4	1	0.54
STN056b.190.fi1.dura.r2	문	26b	74.18	113.34	34.0	-1.2	190	1	1		-	5.4	1	0.54
STN056b.90.pre.poly.3.LG	PA	26b	74.18	113.34	33.9	-1.5	06	1	1		-	5.5	1	0.59
STN056b.90.fil.dura.r1	문	56b	74.18	113.34	33.9	-1.5	06	-	1			5.5	-	0.59
STN056b.90.fil.dura.r2	FL	26b	74.18	113.34	33.9	-1.5	06	-	:			5.5	-	0.59
STN056b.30.pre.poly.3.LG	PA	56b	74.18	113.34	33.8	-1.4	30					9.9		0.50
STN056b.30.fil.dura.r1	Æ	56b	74.18	113.34	33.8	-1.4	30		:			9.9		0.50
STN056b.30.fil.dura.r2	문	26b	74.18	113.34	33.8	-1.4	30	1	1	-	1	9.9	1	0.50
STN068.257.pre.poly.3.LG	PA	89	74.03	113.34	34.1	-0.7	257	33.2	2.23	0.02	0.19	5.1	99	0.51
STN068.257.fil.dura.r1	FL	89	74.03	113.34	34.1	-0.7	257	33.2	2.23	0.02	0.19	5.1	99	0.51
STN068.257.fil.dura.r2	FL	89	74.03	113.34	34.1	-0.7	257	33.2	2.23	0.02	0.19	5.1	99	0.51
STN068.190.pre.poly.3.LG	PA	68	74.03	113.34	34.1	6.0-	190	32.1	2.19	0.02	0.27	5.2	51	0.49
STN068.190.fil.dura.r1	FL	68	74.03	113.34	34.1	6.0-	190	32.1	2.19	0.02	0.27	5.2	51	0.49
STN068.190.fil.dura.r2	FL	68	74.03	113.34	34.1	6.0-	190	32.1	2.19	0.02	0.27	5.2	51	0.49
STN068.90.pre.poly.3.LG	PA	68	74.03	113.34	33.9	-1.3	06	32.1	2.19	0.03	0.09	5.7	44	0.13
STN068.90.fi1.dura.r1	FL	68	74.03	113.34	33.9	-1.4	06	32.1	2.19	0.03	0.09	5.8	44	0.13
STN068.90.fil.dura.r2	FL	89	74.03	113.34	33.9	-1.4	06	32.1	2.19	0.03	60.0	8.8	44	0.13
STN068.30.pre.poly.3.LG	PA	68	74.03	113.34	33.8	-1.0	30	20.9	1.62	0.05	0.19	8.5	45	0.13
STN068.30.fi1.dura.r1	FL	68	74.03	113.34	33.8	-1.0	30	20.9	1.62	0.05	0.19	9.8	45	:
STN068.30.fil.dura.r2	FL	89	74.03	113.34	33.8	-1.0	30	20.9	1.62	0.05	0.19	9.8	45	:
STN078.1040.pre.poly.3.LG	PA	78	74.23	112.69	34.5	0.5	1040	32.9	2.28	0.01	0.24	4.6	40	0.55
STN078.1040.fil.dura.rl	FL	78	74.23	112.69	34.5	0.5	1039	32.9	2.28	0.01	0.24	4.6	40	0.55
STN078.1040.fil.dura.r2	FL	78	74.23	112.69	34.5	0.5	1039	32.9	2.28	0.01	0.24	4.6	40	0.55
STN078.440.pre.poly.3.LG	PA	78	74.23	112.69	34.3	-0.3	440	32.9	2.23	0.01	0.46	5.0	41	0.48
STN078.440.fil.dura.r1	FL	78	74.23	112.69	34.3	-0.3	440	32.9	2.23	0.01	0.46	5.0	41	0.48
STN078.440.fil.dura.r2	FL	78	74.23	112.69	34.3	-0.3	440	32.9	2.23	0.01	0.46	5.0	41	0.48
STN078.300.pre.poly.3.LG	PA	78	74.23	112.69	34.1	-1.4	300	31.7	2.17	0.03	0.13	6.2	-	0.44
STN078.300.fil.dura.r1	FL	78	74.23	112.69	34.1	-1.4	300	31.7	2.17	0.03	0.13	6.2		0.44
STN078.300.fil.dura.r2	FL	78	74.23	112.69	34.1	-1.4	300	31.7	2.17	0.03	0.13	6.2		0.44

	Size		Latitude	Longitude	Practical	Potential	Depth	NO3-	PO4	NO2	NH4	02	DOC	Iron
Sample	Fract.	Station	(deg S)	(deg W)	Salinity	Temp. (°C)	(m)	(µmol/L)	(µmol/L)	(mmol/L)	(µmol/L)	(mL/L)	(µM)	(nmol/kg)
STN078.180.pre.poly.3.LG	PA	78	74.23	112.69	34.0	-1.5	180	30.0	2.09	90.0	0.41	6.3	47	0.36
STN078.100.pre.poly.3.LG	PA	78	74.23	112.69	33.9	-1.4	100	30.5	2.11	0.05	0.41	6.3		0.27
STN078.100.fi1.dura.rl	FL	82	74.23	112.69	33.9	-1.4	100	30.5	2.11	50.0	0.41	6.3		0.27
STN078.100.fil.dura.r2	문	78	74.23	112.69	33.9	-1.4	100	30.5	2.11	0.05	0.41	6.3	:	0.27
STN078.20.pre.poly.3.LG	PA	78	74.23	112.69	33.8	-1.3	20	27.7	1.97	0.05	0.34	7.0	54	0.12
STN078.20.fil.dura.rl	문	78	74.23	112.69	33.8	-1.3	20	27.7	1.97	0.05	0.34	7.1	54	0.12
STN078.20.fil.dura.r2	FL	78	74.23	112.69	33.8	-1.3	20	27.7	1.97	0.05	0.34	7.1	54	0.12
STN089.1271.pre.poly.3.LG	PA	68	74.39	110.09	34.7	1.1	1271	38.6	2.7	0.01	0.48	4.3	44	0.40
STN089.1271.fil.dura.r1	FL	68	74.39	110.09	34.7	1.1	1271	38.6	2.7	0.01	0.48	4.3	44	0.40
STN089.1271.fil.dura.r2	FL	68	74.39	110.09	34.7	1.1	1271	38.6	2.7	0.01	0.48	4.3	44	0.40
STN089.500.pre.poly.3.LG	PA	68	74.39	110.09	34.3	-0.1	500	38.1	2.69	0.01	0.12	4.9	42	0.49
STN089.500.fil.dura.rl	FL	68	74.39	110.09	34.3	-0.1	500	38.1	2.69	0.01	0.12	5.0	42	0.49
STN089.500.fil.dura.r2	FL	68	74.39	110.09	34.3	-0.1	500	38.1	2.69	0.01	0.12	5.0	42	0.49
STN089.300.pre.poly.3.LG	PA	68	74.39	110.09	34.1	8.0-	300	37.5	2.62	0.01	0.13	5.2	41	0.58
STN089.300.fil.dura.rl	FL	68	74.39	110.09	34.1	8.0-	300	37.5	2.62	0.01	0.13	5.2	41	0.58
STN089.300.fil.dura.r2	FL	68	74.39	110.09	34.1	8.0-	300	37.5	2.62	0.01	0.13	5.2	41	0.58
STN089.200.pre.poly.3.LG	PA	68	74.39	110.09	34.0	-1.0	200	37.5	2.59	0.01	0.13	5.3	49	0.63
STN089.200.fil.dura.rl	FL	68	74.39	110.09	34.0	-1.0	200	37.5	2.59	0.01	0.13	5.3	49	0.63
STN089.200.fil.dura.r2	FL	68	74.39	110.09	34.0	-1.0	200	37.5	2.59	0.01	0.13	5.3	49	0.63
STN089.2.pre.poly.3.LG	PA	68	74.39	110.09	33.8	-1.5	2	36.7	2.58	0.02	0.1	5.7	42	0.94
STN089.2.fil.dura.r1	FL	68	74.39	110.09	33.8	-1.5	2	36.7	2.58	0.02	0.1	5.6	42	0.94
STN089.2.fil.dura.r2	FL	68	74.39	110.09	33.8	-1.5	2	36.7	2.58	0.02	0.1	5.7	42	0.94
STN106.318.pre.poly.2.LG	PA	106	74.16	111.44	34.0	-1.4	318	36.4	2.56	0.03	0.17	6.1	40	0.51
STN106.318.fil.dura.rl	FL	106	74.16	111.44	34.0	-1.4	318	36.4	2.56	0.03	0.17	6.0	40	0.51
STN106.318.fi1.dura.r2	FL	106	74.16	111.44	34.0	-1.4	318	36.4	2.56	0.03	0.17	6.0	40	0.51
STN106.200.pre.poly.3.S	PA	106	74.16	111.44	34.0	-1.4	200	36.2	2.51	0.04	0.22	6.0		
STN106.200.fil.dura.rl	FL	106	74.16	111.44	34.0	-1.4	200	36.2	2.51	0.04	0.22	0.9	1	;
STN106.200.fi1.dura.r2	표	106	74.16	111.44	34.0	-1.4	200	36.2	2.51	0.04	0.22	0.9	1	;
STN106.170.pre.poly.2.LG	PA	106	74.16	111.44	34.0	-1.3	170	36.5	2.56	0.04	0.35	5.8	42	0.52
STN106.170.fil.dura.rl	FL	106	74.16	111.44	34.0	-1.3	170	36.5	2.56	0.04	0.35	5.8	42	0.52
STN106.170.fi1.dura.r2	FL	106	74.16	111.44	34.0	-1.3	170	36.5	2.56	0.04	0.35	5.8	42	0.52

	Size		Latitude	Longitude	Practical	Potential	Depth	NO3-	PO4	NO2	NH4	02	DOC	Iron
Sampie	Fract.	мапоп	(deg S)	(deg W)	Salinity	Temp. (°C)	(m)	(µmol/L)	(µmol/L)	(µmol/L)	(µmol/L)	(mL/L)	(μM)	(nmol/kg)
STN106.100.pre.poly.3.S	PA	106	74.16	111.44	33.9	-1.4	100	35.1	2.49	0.03	0.23	6.1	43	0.51
STN106.100.fil.dura.r1	ТЫ	106	74.16	111.44	33.9	-1.4	100	35.1	2.49	0.03	0.23	6.1	43	0.51
STN106.100.fil.dura.r2	ТЫ	106	74.16	111.44	33.9	-1.4	100	35.1	2.49	0.03	0.23	6.1	43	0.51
STN106.20.pre.poly.3.S	PA	106	74.16	111.44	33.8	-1.3	20	32.6	2.27	0.05	0.16	6.9	42	0.17
STN106.20.fil.dura.r1	ЪГ	106	74.16	111.44	33.8	-1.3	20	32.6	2.27	50.0	0.16	0.7	42	0.17
STN106.20.fil.dura.r2	FL	106	74.16	111.44	33.8	-1.3	20	32.6	2.27	0.05	0.16	7.0	42	0.17
STN115.730.pre.poly.3.S	PA	115	73.80	112.67	34.6	9.0	730	37.4	2.74	0.02	0.19	4.6	51	86.0
STN115.730.fil.dura.r1	ТЫ	115	73.80	112.67	34.6	9.0	730	37.4	2.74	0.02	0.19	4.6	51	86.0
STN115.730.fil.dura.r2	FL	115	73.80	112.67	34.6	9.0	300	37.4	2.74	0.02	0.19	0.9	51	86.0
STN115.300.pre.poly.3.S	PA	115	73.80	112.67	34.2	-1.1	300	35.6	2.61	0.02	0.22	0.9	43	:
STN115.300.fil.dura.r1	ТЫ	115	73.80	112.67	34.2	-1.1	300	35.6	2.61	0.02	0.22	0.9	43	:
STN115.300.fil.dura.r2	ТЫ	115	73.80	112.67	34.2	-1.1	300	35.6	2.61	0.02	0.22	0.9	43	
STN115.180.pre.poly.3.S	PA	115	73.80	112.67	34.0	-1.4	180	35.1	2.6	20.0	0.34	6.2	09	
STN115.180.fil.dura.rl	Ъ	115	73.80	112.67	34.0	-1.4	180	35.1	2.6	20.0	0.34	6.2	09	
STN115.180.fil.dura.r2	ЪГ	115	73.80	112.67	34.0	-1.4	180	35.1	2.6	20.0	0.34	6.2	09	-
STN115.125.pre.poly.3.S	ΡA	115	73.80	112.67	33.9	-1.3	125	34.7	2.55	0.05	0.52	0.9	46	
STN115.125.fil.dura.rl	FL	115	73.80	112.67	33.9	-1.3	125	34.7	2.55	0.05	0.52	5.9	46	
STN115.125.fil.dura.r2	FL	115	73.80	112.67	33.9	-1.3	125	34.7	2.55	0.05	0.52	5.9	46	:
STN115.35.pre.poly.3.S	PA	115	73.80	112.67	33.8	-1.0	35	23.0	1.92	0.06	0.59	8.3	48	
STN115.35.fil.dura.rl	Ъ	115	73.80	112.67	33.8	6.0-	35	23.0	1.92	90.0	0.59	8.3	48	
STN115.35.fil.dura.r2	HL	115	73.80	112.67	33.8	6.0-	35	23.0	1.92	90.0	0.59	8.3	48	-
STN132.505.pre.poly.3.S	PA	132	74.20	110.9	34.1	-1.3	505	32.2	2.19	0.01	0.21	0.9	49	0.53
STN132.505.fil.dura.r1	FL	132	74.20	110.9	34.1	-1.3	505	32.2	2.19	0.01	0.21	0.9	49	0.53
STN132.505.fil.dura.r2	FL	132	74.20	110.9	34.1	-1.3	505	32.2	2.19	0.01	0.21	0.9	49	0.53
STN132.305.pre.poly.3.S	PA	132	74.20	110.9	34.1	-1.3	305	32.1	2.17	0.02	0.09	0.9	42	0.53
STN132.305.fil.dura.r1	FL	132	74.20	110.9	34.1	-1.3	305	32.1	2.17	0.02	0.09	0.9	42	0.53
STN132.305.fil.dura.r2	FL	132	74.20	110.9	34.1	-1.3	305	32.1	2.17	0.02	0.09	6.0	42	0.53
STN132.200.pre.poly.3.S	PA	132	74.20	110.9	34.0	-1.2	200	32.2	2.17	0.02	0.14	5.6	43	0.59
STN132.200.fil.steri.r1	FL	132	74.20	110.9	34.0	-1.2	200	32.2	2.17	0.02	0.14	5.7	43	0.59
STN132.200.fil.dura.r2	HL	132	74.20	110.9	34.0	-1.2	200	32.2	2.17	0.02	0.14	5.7	43	0.59
STN132.100.pre.poly.3.S	PA	132	74.20	110.9	33.9	-1.4	100	32.2	2.19	0.01	0.24	5.6	47	0.55

i	Size		Latitude	Longitude	Practical	Potential	Depth	NO3-	PO4	NO2	NH4	02	DOC	Iron
Sample	Fract.	Station	(deg S)	(deg W)	Salinity	Temp. (°C)	(m)	(µmol/L)	(µmol/L)	$(\mu mol/L)$	(µmol/L)	(mL/L)	(μM)	(nmol/kg)
STN132.100.fil.steri.r1	H	132	74.20	110.9	33.9	-1.4	100	32.2	2.19	0.01	0.24	5.6	47	0.55
STN132.100.fil.steri.r2	FL	132	74.20	110.9	33.9	-1.4	100	32.2	2.19	0.01	0.24	5.6	47	0.55
STN132.30.pre.poly.3.S	PA	132	74.20	110.9	33.8	-1.4	30	31.6	2.12	0.02	0.2	6.2	49	0.45
STNI 32.30.fil.steri.rl	FL	132	74.20	110.9	33.8	-1.4	30	31.6	2.12	0.02	0.2	6.2	49	0.45
STN132.30.fil.steri.r2	FL	132	74.20	110.9	33.8	-1.4	30	31.6	2.12	0.02	0.2	6.2	49	0.45
STN146.268.pre.poly.3.S	PA	146	73.86	114.02	34.1	6.0-	268	32.8	2.25	0.03	0.33	5.3	43	0.61
STN146.268.fil.steri.rl	FL	146	73.86	114.02	34.1	8.0-	268	32.8	2.25	0.03	0.33	5.3	43	0.61
STN146.268.fil.steri.r2	FL	146	73.86	114.02	34.1	-0.8	268	32.8	2.25	0.03	0.33	5.3	43	0.61
STN146.250.pre.poly.3.S	PA	146	73.86	114.02	34.1	6.0-	250	32.0	2.19	0.04	0.17	5.3	43	0.57
STN146.250.fi1.poly.S.r1	FL	146	73.86	114.02	34.1	6.0-	250	32.0	2.19	0.04	0.17	5.3	43	0.57
STN146.201.pre.poly.3.S	PA	146	73.86	114.02	34.0	-1.1	201	32.3	2.22	0.05	0.5	5.5	49	0.54
STN146.201.fil.steri.r1	FL	146	73.86	114.02	34.0	-1.1	201	32.3	2.22	0.05	0.5	5.5	49	0.54
STN146.201.fil.steri.r2	FL	146	73.86	114.02	34.0	-1.1	200	32.3	2.22	0.05	0.5	5.5	62	0.54
STN146.160.pre.poly.3.S	PA	146	73.86	114.02	33.9	-1.2	160	30.3	2.13	0.05	0.63	0.9	62	0.48
STN146.160.fi1.poly.S.r1	FL	146	73.86	114.02	33.9	-1.2	160	30.3	2.13	0.05	0.63	0.9	62	0.48
STN146.30.pre.poly.3.S	PA	146	73.86	114.02	33.8	-1.0	30	18.5	1.54	0.07	0.51	9.8	09	0.14
STN146.30.fil.steri.r1	FL	146	73.86	114.02	33.8	-1.0	30	18.5	1.54	0.07	0.51	9.8	09	0.14
STN146.30.fil.steri.r2	FL	146	73.86	114.02	33.8	-1.0	30	18.5	1.54	0.07	0.51	8.6	09	0.14
STN153.548.pre.poly.3.S	PA	153	73.92	118.84	34.4	0.0	548	33.2	2.27	0.02	0.03	5.0	38	0.80
STN153.548.fil.poly.Lr1	FL	153	73.92	118.84	34.4	0.0	548	33.2	2.27	0.02	0.03	5.0	38	0.80
STN153.300.fi1.poly.Lr1	FL	153	73.92	118.84	34.1	-1.7	300	33.2	2.27	0.02	0.03	6.3		0.28
STN153.200.fi1.poly.Lr1	FL	153	73.92	118.84	34.0	-1.4	200	32.4	2.23	0.04	0.15	5.7	1	0.42
STN153.160.pre.poly.3.S	PA	153	73.92	118.84	34.0	-1.4	160	31.6	2.17	0.02	0.13	5.8	38	0.38
STN153.160.fi1.poly.S.r1	FL	153	73.92	118.84	34.0	-1.4	160	31.6	2.17	0.02	0.13	5.8	46	0.38
STN153.120.fi1.poly.S.r1	FL	153	73.92	118.84	33.9	-1.3	120	31.6	2.17	0.02	0.13	6.3	44	0.38
STN153.2.pre.poly.3.S	PA	153	73.92	118.84	33.8	-0.3	2	11.0	1.13	0.1	0.64	9.1	52	0.26
STN153.2.fi1.poly.S	FL	153	73.92	118.84	33.8	-0.3	2	11.0	1.13	0.1	0.64	9.1	52	0.26
STN12.3.732.pre.poly.3.S	PA	12.3	73.80	112.67	34.6	0.5	732	36.5	2.68	0.02	0.23	4.6	44	-
STN12.3.732.fil.poly.S.r1	FL	12.3	73.80	112.67	34.6	0.5	731	36.5	2.68	0.02	0.23	4.6	44	-
STN12.3.300.pre.poly.3.S	PA	12.3	73.80	112.67	34.2	-1.1	300	35.3	2.58	0.03	0.29	5.9	46	;
STN12.3.300.fil.poly.S.r1	FL	12.3	73.80	112.67	34.2	-1.1	300	35.3	2.58	0.03	0.29	5.9	46	;

	Size	:	Latitude	Longitude	Practical	Potential	Depth	NO3-	PO4	NO2	NH4	02	DOC	Iron
Sample	Fract.	Station	(deg S)	(deg W)	Salinity	Temp. (°C)	(m)	(µmol/L)	(µmol/L)	(µmol/L)	(µmol/L)	(mL/L)	(μM)	(nmol/kg)
STN12.3.165.pre.poly.3.S	PA	12.3	73.80	112.67	34.0	-1.5	165	34.1	2.52	0.07	19:0	6.2	40	:
STN12.3.165.fil.poly.S.r1	FL	12.3	73.80	112.67	34.0	-1.4	165	34.1	2:22	0.07	29.0	6.2	40	:
STN12.3.15.pre.poly.3.S	PA	12.3	73.80	112.67	33.8	6.0-	15	17.71	1.6	0.07	0.73	8.7	51	+
STN12.3.15.fil.poly.Sr1	FL	12.3	73.80	112.67	33.8	6.0-	15	17.7	1.6	0.07	0.73	8.7	51	;
STN151.2.673.pre.poly.3.S	PA	151.2	73.88	118.74	34.5	0.4	673	33.5	2.26	0.01	0.26	4.8	44	0.53
STN151.2.673.fil.poly.S.r1	FL	151.2	73.88	118.74	34.5	0.4	673	33.5	2.26	0.01	0.26	4.7	44	0.53
STN151.2.600.pre.poly.3.S	PA	151.2	73.88	118.74	34.5	0.3	009	33.5	2.28	0.01	0.16	4.8		-
STN151.2.600.fil.poly.S.r1	FL	151.2	73.88	118.74	34.5	0.3	009	33.5	2.28	0.01	0.16	4.8		:
STN151.2.500.pre.poly.3.S	PA	151.2	73.88	118.74	34.3	-0.3	500	33.2	2.28	0.01	0.13	5.1	42	-
STN151.2.500.fil.poly.S.r1	FL	151.2	73.88	118.74	34.3	-0.3	500	33.2	2.28	0.01	0.13	5.1	42	:
STN174.620.pre.poly.3.S	PA	174	73.73	116.85	34.5	0.1	620	33.1	2.29	0.04	0.28	4.9	45	0.87
STN174.620.fil.poly.S.rl	FL	174	73.73	116.85	34.5	0.1	620	33.1	2.29	0.04	0.28	4.8	45	0.87
STN174.550.pre.poly.3.S	PA	174	73.73	116.85	34.4	-0.2	550	33.3	2.3	0.05	0.16	5.0	54	0.75
STN174.550.fil.poly.S.rl	FL	174	73.73	116.85	34.4	-0.2	550	33.3	2.3	0.05	0.16	5.0	54	0.75
STN174.280.pre.poly.3.S	PA	174	73.73	116.85	34.1	-1.8	280	31.5	2.2	0.17	0.5	6.5		0.33
STN174.280.fil.poly.S.r1	FL	174	73.73	116.85	34.1	-1.8	280	31.5	2.2	0.17	0.5	6.5		0.33
STN174.3.pre.poly.3.S	PA	174	73.73	116.85	33.7	0.0	3	3.8	89.0	0.07	0.34	2.8	92	0.11
STN174.3.fil.poly.S.rl	FL	174	73.73	116.85	33.7	0.0	3	3.8	89.0	0.07	0.34	8.7	92	0.11
STN181.757.pre.poly.3.S	PA	181	73.42	114.21	34.6	9.0	757	33.6	2.31	0.04	0.31	4.5		:
STN181.757.fil.poly.S.r1	FL	181	73.42	114.21	34.6	9.0	757	33.6	2.31	0.04	0.31	4.5		:
STN181.340.pre.poly.3.S	PA	181	73.42	114.21	34.1	-1.7	340	31.8	2.18	0.16	0.51	6.5		-
STN181.340.fil.poly.S.r1	FL	181	73.42	114.21	34.1	-1.7	340	31.8	2.18	0.16	0.51	6.5	-	;
STN181.2.pre.poly.3.S	PA	181	73.42	114.21	33.8	-1.3	2	18.9	1.51	0.08	0.36	8.7	-	:
STN181.2.fil.poly.S.rl	FL	181	73.42	114.21	33.8	-1.3	2	18.9	1.51	0.08	0.36	8.7	-	1
STN198.20.pre.poly.3.S	PA	198	72.00	119.4	33.3	-1.1	20	13.6	1.19	0.09	2.07	8.4	58	0.16
STN198.1487.pre.poly.3.S	PA	198	72.00	119.4	34.7	9.0	1487	33.6	2.27	0.02	0.19	4.7	44	0.58
STN198.1487.fil.poly.LGr2	FL	198	72.00	119.4	34.7	9.0	1486	33.6	2.27	0.02	0.19	4.7	44	0.58
STN198.750.fil.poly.LGr1	FL	198	72.00	119.4	34.7	1.2	750	33.2	2.21	0.01	0.12	4.5	1	0.36
STN198.376.pre.poly.3.S	PA	198	72.00	119.4	34.7	1.7	376	33.5	2.26	0.02	0.16	4.2	44	0.44
STN198.376.fil.poly.S.r2	FL	198	72.00	119.4	34.7	1.7	376	33.5	2.26	0.02	0.16	4.2	44	0.44
STN198.300.pre.poly.3.S	PA	198	72.00	119.4	34.6	6.0	300	33.9	2.3	0.05	0.15	4.5	-	0.31

.[	Size	24.04.0	Latitude	Longitude	Practical	Longitude Practical Potential Depth	Depth	NO3-	PO4	NO2	NH4	02	DOC	Iron
Sampre	Fract.	Station	(deg S)	(deg W)		Salinity Temp. (°C) (m)	(m)	$(\mu mol/L)$	(mmol/L)	$(\mu mol/L)$	(mmol/L)	(mL/L)	(μM)	(nmol/kg)
STN198.300.fil.poly.S.r1		FL 198	72.00	119.4	34.6	6.0	300	33.9	2.3	50.0	0.15	4.5		0.31
STN198.150.pre.poly.3.LG PA 198	PA	198	72.00	119.4	34.1	-1.7	150	31.6	2.17	20.0	6.0	6.4		0.25
STN198.150.fil.poly.LG.r1		FL 198	72.00	119.4	34.1	-1.7	150	31.6	2.17	70.0	6.0	6.4	-	0.25